Thus, it is expected that MN4/LSDQgtu will grow much better in RhM individuals, at least in the early infection phase, than the other HIV-1mt clones constructed. As reported previously, the replication of HIV-1 derivatives in infected macaques was eventually controlled, and no disease was induced in the animals (16, 20, 21, 24, 64). It has been suggested that the replication ability of primate lentiviruses in unusual hosts is more severely affected, via an interferon-induced antiviral state mediated by unidentified species-specific factors, than that in natural hosts (23). Moreover, there are the other significant issues to be considered, such as viral coreceptor tropism (CXCR4 versus CCR5), the diversity in viral growth properties (HIV-1 versus SIVmac), and the difference in host immune responses (human versus RhM) (9, 65–67). Most importantly, CCR5-tropic but not CXCR4-tropic clones have been found to be appropriate as input viruses to experimentally infect RhMs for various HIV-1 model studies *in vivo* (65–67). Although MN4/LSDQgtu is a CXCR4-tropic virus, it has clear potential for the establishment of a model system. MN4/LSDQgtu can be changed to a pathogenic CCR5-tropic virus through *in vitro* and *in vivo* approaches, as well documented by previous SHIV studies (68–70). It is also possible to generate entirely new CCR5-tropic HIV-1mt clones other than MN4/LSDQgtu derivatives on the basis of the key findings for Gag-CA and Vpu-TM in this study.

Our study here describes the generation and characterization of a novel HIV-1 derivative minimally chimeric with SIVs. Several infection model systems using distinct viruses and nonhuman primates are now available. It is important to define common and unique characteristics of each virus-host interaction based on the results obtained from various experimental approaches, including SIV/natural host and SIVmac/RhM, SHIV/RhM, and HIV-1mt/RhM infection systems. Such efforts would shed light on a better understanding of HIV-1/human infection and HIV-1 pathogenesis.

ACKNOWLEDGMENTS

This study was supported in part by a grant from the Ministry of Health, Labor and Welfare of Japan (Research on HIV/AIDS project no. H23-003).

We thank Kazuko Yoshida for editorial assistance.

We declare that no competing interests exist.

REFERENCES

1. **Kirchhoff F.** 2010. Immune evasion and counteraction of restriction factors by HIV-1 and other primate lentiviruses. Cell Host Microbe **8**:55–67.
2. **Sharp PM, Hahn BH.** 2011. Origins of HIV and the AIDS pandemic. Cold Spring Harb. Perspect. Med. **1**:a006841. doi:10.1101/cshperspect.a006841.
3. **Shibata R, Sakai H, Kawamura M, Tokunaga K, Adachi A.** 1995. Early replication block of human immunodeficiency virus type 1 in monkey cells. J. Gen. Virol. **76**:2723–2730.
4. **Blanco-Melo D, Venkatesh S, Bieniasz PD.** 2012. Intrinsic cellular defenses against human immunodeficiency viruses. Immunity **37**:399–411.
5. **Harris RS, Hultquist JF, Evans DT.** 2012. The restriction factors of human immunodeficiency virus. J. Biol. Chem. **287**:40875–40883.
6. **Malim MH, Bieniasz PD.** 2012. HIV restriction factors and mechanisms of evasion. Cold Spring Harb. Perspect. Med. **2**:a006940. doi:10.1101/cshperspect.a006940.
7. **Hatziioannou T, Evans DT.** 2012. Animal models for HIV/AIDS research. Nat. Rev. Microbiol. **10**:852–867.
8. **Nomaguchi M, Doi N, Fujiwara S, Adachi A.** 2011. Macaque-tropic HIV-1 derivatives: a novel experimental approach to understand viral replication and evolution *in vivo*, p 325–348. *In* Chang T.Y.-L. (ed), HIV-host interactions. InTech, Rijeka, Croatia. http://www.intechopen.com/books/hiv-host-interactions/macaque-tropic-hiv-1-derivatives-a-novel-experimental-approach-to-understand-viral-replication-and-e.
9. **Shedlock DJ, Silvestri G, Weiner DB.** 2009. Monkeying around with HIV vaccines: using rhesus macaques to define 'gatekeepers' for clinical trials. Nat. Rev. Immunol. **9**:717–728.
10. **Nomaguchi M, Doi N, Matsumoto Y, Sakai Y, Fujiwara S, Adachi A.** 2012. Species tropism of HIV-1 modulated by viral accessory proteins. Front. Microbiol. **3**:267. doi:10.3389/fmicb.2012.00267.
11. **Holmes RK, Malim MH, Bishop KN.** 2007. APOBEC-mediated viral restriction: not simply editing? Trends Biochem. Sci. **32**:118–128.
12. **Malim MH, Emerman M.** 2008. HIV-1 accessory proteins—ensuring viral survival in a hostile environment. Cell Host Microbe **3**:388–398.
13. **Grütter MG, Luban J.** 2012. TRIM5 structure, HIV-1 capsid recognition, and innate immune signaling. Curr. Opin. Virol. **2**:142–150.
14. **Nakayama EE, Shioda T.** 2010. Anti-retroviral activity of TRIM5 alpha. Rev. Med. Virol. **20**:77–92.
15. **Douglas JL, Gustin JK, Viswanathan K, Mansouri M, Moses AV, Früh K.** 2010. The great escape: viral strategies to counter BST-2/tetherin. PLoS Pathog. **6**:e1000913. doi:10.1371/journal.ppat.1000913.
16. **Hatziioannou T, Ambrose Z, Chung NP, Piatak M, Jr, Yuan F, Trubey CM, Coalter V, Kiser R, Schneider D, Smedley J, Pung R, Gathuka M, Estes JD, Veazey RS, KewalRamani VN, Lifson JD, Bieniasz PD.** 2009. A macaque model of HIV-1 infection. Proc. Natl. Acad. Sci. U. S. A. **106**:4425–4429.
17. **Hatziioannou T, Princiotta M, Piatak M, Jr, Yuan F, Zhang F, Lifson JD, Bieniasz PD.** 2006. Generation of simian-tropic HIV-1 by restriction factor evasion. Science **314**:95. doi:10.1126/science.1130994.
18. **Kamada K, Igarashi T, Martin MA, Khamsri B, Hatcho K, Yamashita T, Fujita M, Uchiyama T, Adachi A.** 2006. Generation of HIV-1 derivatives that productively infect macaque monkey lymphoid cells. Proc. Natl. Acad. Sci. U. S. A. **103**:16959–16964.
19. **Nomaguchi M, Yokoyama M, Kono K, Nakayama EE, Shioda T, Saito A, Akari H, Yasutomi Y, Matano T, Sato H, Adachi A.** 2013. Gag-CA Q110D mutation elicits TRIM5-independent enhancement of HIV-1mt replication in macaque cells. Microbes Infect. **15**:56–65.
20. **Saito A, Nomaguchi M, Iijima S, Kuroishi A, Yoshida T, Lee YJ, Hayakawa T, Kono K, Nakayama EE, Shioda T, Yasutomi Y, Adachi A, Matano T, Akari H.** 2011. Improved capacity of a monkey-tropic HIV-1 derivative to replicate in cynomolgus monkeys with minimal modifications. Microbes Infect. **13**:58–64.
21. **Thippeshappa R, Polacino P, Yu Kimata MT, Siwak EB, Anderson D, Wang W, Sherwood L, Arora R, Wen M, Zhou P, Hu SL, Kimata JT.** 2011. Vif substitution enables persistent infection of pig-tailed macaques by human immunodeficiency virus type 1. J. Virol. **85**:3767–3779.
22. **Shingai M, Yoshida T, Martin MA, Strebel K.** 2011. Some human immunodeficiency virus type 1 Vpu proteins are able to antagonize macaque BST-2 *in vitro* and *in vivo*: Vpu-negative simian-human immunodeficiency viruses are attenuated *in vivo*. J. Virol. **85**:9708–9715.
23. **Bitzegeio J, Sampias M, Bieniasz PD, Hatziioannou T.** 2013. Adaptation to the interferon-induced antiviral state by human and simian immunodeficiency viruses. J. Virol. **87**:3549–3560.
24. **Saito A, Nomaguchi M, Kono K, Iwatani Y, Yokoyama M, Yasutomi Y, Sato H, Shioda T, Sugiura W, Matano T, Adachi A, Nakayama E, Akari H.** 2013. *TRIM5* genotypes in cynomolgus monkeys primarily influence inter-individual diversity in susceptibility to monkey-tropic human immunodeficiency virus type 1. J. Gen. Virol. **94**:1318–1324.
25. **Doi N, Fujiwara S, Adachi A, Nomaguchi M.** 2011. Rhesus M1.3S cells suitable for biological evaluation of macaque-tropic HIV/SIV clones. Front. Microbiol. **2**:115. doi:10.3389/fmicb.2011.00115.
26. **Sauter D, Schindler M, Specht A, Landford WN, Münch J, Kim KA, Votteler J, Schubert U, Bibollet-Ruche F, Keele BF, Takehisa J, Ogando Y, Ochsenbauer C, Kappes JC, Ayouba A, Peeters M, Learn GH, Shaw G, Sharp PM, Bieniasz P, Hahn BH, Hatziioannou T, Kirchhoff F.** 2009. Tetherin-driven adaptation of Vpu and Nef function and the evolution of pandemic and nonpandemic HIV-1 strains. Cell Host Microbe **6**:409–421.
27. **Lebkowski JS, Clancy S, Calos MP.** 1985. Simian virus 40 replication in adenovirus-transformed human cells antagonizes gene expression. Nature **317**:169–171.
28. **Kimpton J, Emerman M.** 1992. Detection of replication-competent and pseudotyped human immunodeficiency virus with a sensitive cell line on the basis of activation of an integrated beta-galactosidase gene. J. Virol. **66**:2232–2239.
29. **Nomaguchi M, Doi N, Fujiwara S, Fujita M, Adachi A.** 2010. Site-

directed mutagenesis of HIV-1 *vpu* gene demonstrates two clusters of replication-defective mutants with distinct ability to down-modulate cell surface CD4 and tetherin. Front. Microbiol. 1:116. doi:10.3389/fmicb.2010.00116.

30. McNatt MW, Zang T, Hatziioannou T, Bartlett M, Fofana IB, Johnson WE, Neil SJ, Bieniasz PD. 2009. Species-specific activity of HIV-1 Vpu and positive selection of tetherin transmembrane domain variants. PLoS Pathog. 5:e1000300. doi:10.1371/journal.ppat.1000300.
31. Yoshida T, Kao S, Strebel K. 2011. Identification of residues in the BST-2 TM domain important for antagonism by HIV-1 Vpu using a gain-of-function approach. Front. Microbiol. 2:35. doi:10.3389/fmicb.2011.00035.
32. Adachi A, Gendelman HE, Koenig S, Folks T, Willey R, Rabson A, Martin MA. 1986. Production of acquired immunodeficiency syndrome-associated retrovirus in human and nonhuman cells transfected with an infectious molecular clone. J. Virol. 59:284–291.
33. Willey RL, Smith DH, Lasky LA, Theodore TS, Earl PL, Moss B, Capon DJ, Martin MA. 1988. In vitro mutagenesis identifies a region within the envelope gene of the human immunodeficiency virus that is critical for infectivity. J. Virol. 62:139–147.
34. O'Doherty U, Swiggard WJ, Malim MH. 2000. Human immunodeficiency virus type 1 spinoculation enhances infection through virus binding. J. Virol. 74:10074–10080.
35. Wilson SJ, Webb BL, Ylinen LM, Verschoor E, Heeney JL, Towers GJ. 2008. Independent evolution of an antiviral TRIMCyp in rhesus macaques. Proc. Natl. Acad. Sci. U. S. A. 105:3557–3562.
36. Kono K, Song H, Yokoyama M, Sato H, Shioda T, Nakayama EE. 2010. Multiple sites in the N-terminal half of simian immunodeficiency virus capsid protein contribute to evasion from rhesus monkey TRIM5α-mediated restriction. Retrovirology 7:72. doi:10.1186/1742-4690-7-72.
37. Howard BR, Vajdos FF, Li S, Sundquist WI, Hill CP. 2003. Structural insights into the catalytic mechanism of cyclophilin A. Nat. Struct. Biol. 10:475–481.
38. Park SH, Mrse AA, Nevzorov AA, Mesleh MF, Oblatt-Montal M, Montal M, Opella SJ. 2003. Three-dimensional structure of the channel-forming trans-membrane domain of virus protein "u" (Vpu) from HIV-1. J. Mol. Biol. 333:409–424.
39. Leaver-Fay A, Tyka M, Lewis SM, Lange OF, Thompson J, Jacak R, Kaufman K, Renfrew PD, Smith CA, Sheffler W, Davis IW, Cooper S, Treuille A, Mandell DJ, Richter F, Ban YE, Fleishman SJ, Corn JE, Kim DE, Lyskov S, Berrondo M, Mentzer S, Popović Z, Havranek JJ, Karanicolas J, Das R, Meiler J, Kortemme T, Gray JJ, Kuhlman B, Baker D, Bradley P. 2011. ROSETTA3: an object-oriented software suite for the simulation and design of macromolecules. Methods Enzymol. 487:545–574.
40. Kirmaier A, Wu F, Newman RM, Hall LR, Morgan JS, O'Connor S, Marx PA, Meythaler M, Goldstein S, Buckler-White A, Kaur A, Hirsch VM, Johnson WE. 2010. *TRIM5* suppresses cross-species transmission of a primate immunodeficiency virus and selects for emergence of resistant variants in the new species. PLoS Biol. 8:e1000462. doi:10.1371/journal.pbio.1000462.
41. Newman RM, Hall L, Connole M, Chen GL, Sato S, Yuste E, Diehl W, Hunter E, Kaur A, Miller GM, Johnson WE. 2006. Balancing selection and the evolution of functional polymorphism in Old World monkey TRIM5alpha. Proc. Natl. Acad. Sci. U. S. A. 103:19134–19139.
42. Price AJ, Marzetta F, Lammers M, Ylinen LM, Schaller T, Wilson SJ, Towers GJ, James LC. 2009. Active site remodeling switches HIV specificity of antiretroviral TRIMCyp. Nat. Struct. Mol. Biol. 16:1036–1042.
43. Ylinen LM, Price AJ, Rasaiyaah J, Hué S, Rose NJ, Marzetta F, James LC, Towers GJ. 2010. Conformational adaptation of Asian macaque TRIMCyp directs lineage specific antiviral activity. PLoS Pathog. 6:e1001062. doi:10.1371/journal.ppat.1001062.
44. Fassati A. 2012. Multiple roles of the capsid protein in the early steps of HIV-1 infection. Virus Res. 170:15–24.
45. Ganser-Pornillos BK, Yeager M, Sundquist WI. 2008. The structural biology of HIV assembly. Curr. Opin. Struct. Biol. 18:203–217.
46. Miyamoto T, Yokoyama M, Kono K, Shioda T, Sato H, Nakayama EE. 2011. A single amino acid of human immunodeficiency virus type 2 capsid protein affects conformation of two external loops and viral sensitivity to TRIM5α. PLoS One 6:e22779. doi:10.1371/journal.pone.0022779.
47. Nomaguchi M, Doi N, Fujiwara S, Saito A, Akari H, Nakayama EE, Shioda T, Yokoyama M, Sato H, Adachi A. 2013. Systemic biological analysis of the mutations in two distinct HIV-1mt genomes occurred during replication in macaque cells. Microbes Infect. 15:319–328.
48. Hatziioannou T, Cowan S, Von Schwedler UK, Sundquist WI, Bieniasz PD. 2004. Species-specific tropism determinants in the human immunodeficiency virus type 1 capsid. J. Virol. 78:6005–6012.
49. Owens CM, Song B, Perron MJ, Yang PC, Stremlau M, Sodroski J. 2004. Binding and susceptibility to postentry restriction factors in monkey cells are specified by distinct regions of the human immunodeficiency virus type 1 capsid. J. Virol. 78:5423–5437.
50. von Schwedler UK, Stray KM, Garrus JE, Sundquist WI. 2003. Functional surfaces of the human immunodeficiency virus type 1 capsid protein. J. Virol. 77:5439–5450.
51. Lim SY, Rogers T, Chan T, Whitney JB, Kim J, Sodroski J, Letvin NL. 2010. TRIM5alpha modulates immunodeficiency virus control in rhesus monkeys. PLoS Pathog. 6:e1000738. doi:10.1371/journal.ppat.1000738.
52. Jia B, Serra-Moreno R, Neidermyer W, Rahmberg A, Mackey J, Fofana IB, Johnson WE, Westmoreland S, Evans DT. 2009. Species-specific activity of SIV Nef and HIV-1 Vpu in overcoming restriction by tetherin/BST2. PLoS Pathog. 5:e1000429. doi:10.1371/journal.ppat.1000429.
53. Zhang F, Wilson SJ, Landford WC, Virgen B, Gregory D, Johnson MC, Munch J, Kirchhoff F, Bieniasz PD, Hatziioannou T. 2009. Nef proteins from simian immunodeficiency viruses are tetherin antagonists. Cell Host Microbe 6:54–67.
54. Vigan R, Neil SJ. 2010. Determinants of tetherin antagonism in the transmembrane domain of the human immunodeficiency virus type 1 Vpu protein. J. Virol. 84:12958–12970.
55. McCarthy KR, Schmidt AG, Kirmaier A, Wyand AL, Newman RM, Johnson WE. 2013. Gain-of-sensitivity mutations in a Trim5-resistant primary isolate of pathogenic SIV identify two independent conserved determinants of Trim5α specificity. PLoS Pathog. 9:e1003352. doi:10.1371/journal.ppat.1003352.
56. Kuroishi A, Saito A, Shingai Y, Shioda T, Nomaguchi M, Adachi A, Akari H, Nakayama EE. 2009. Modification of a loop sequence between alpha-helices 6 and 7 of virus capsid (CA) protein in a human immunodeficiency virus type 1 (HIV-1) derivative that has simian immunodeficiency virus (SIVmac239) vif and CA alpha-helices 4 and 5 loop improves replication in cynomolgus monkey cells. Retrovirology 6:70. doi:10.1186/1742-4690-6-70.
57. Ohkura S, Goldstone DC, Yap MW, Holden-Dye K, Taylor IA, Stoye JP. 2011. Novel escape mutants suggest an extensive TRIM5α binding site spanning the entire outer surface of the murine leukemia virus capsid protein. PLoS Pathog. 7:e1002011. doi:10.1371/journal.ppat.1002011.
58. Homann S, Smith D, Little S, Richman D, Guatelli J. 2011. Upregulation of BST-2/tetherin by HIV infection *in vivo*. J. Virol. 85:10659–10668.
59. Liberatore RA, Bieniasz PD. 2011. Tetherin is a key effector of the antiretroviral activity of type I interferon in vitro and in vivo. Proc. Natl. Acad. Sci. U. S. A. 108:18097–18101.
60. Pillai SK, Abdel-Mohsen M, Guatelli J, Skasko M, Monto A, Fujimoto K, Yukl S, Greene WC, Kovari H, Rauch A, Fellay J, Battegay M, Hirschel B, Witteck A, Bernasconi E, Ledergerber B, Günthard HF, Wong JK, Swiss HIV Cohort Study. 2012. Role of retroviral restriction factors in the interferon-α-mediated suppression of HIV-1 in vivo. Proc. Natl. Acad. Sci. U. S. A. 109:3035–3040.
61. Serra-Moreno R, Jia B, Breed M, Alvarez X, Evans DT. 2011. Compensatory changes in the cytoplasmic tail of gp41 confer resistance to tetherin/BST-2 in a pathogenic nef-deleted SIV. Cell Host Microbe 9:46–57.
62. Goldstein S, Brown CR, Dehghani H, Lifson JD, Hirsch VM. 2000. Intrinsic susceptibility of rhesus macaque peripheral CD4(+) T cells to simian immunodeficiency virus in vitro is predictive of in vivo viral replication. J. Virol. 74:9388–9395.
63. Lifson JD, Nowak MA, Goldstein S, Rossio JL, Kinter A, Vasquez G, Wiltrout TA, Brown C, Schneider D, Wahl L, Lloyd AL, Williams J, Elkins WR, Fauci AS, Hirsch VM. 1997. The extent of early viral replication is a critical determinant of the natural history of simian immunodeficiency virus infection. J. Virol. 71:9508–9514.
64. Igarashi T, Iyengar R, Byrum RA, Buckler-White A, Dewar RL, Buckler CE, Lane HC, Kamada K, Adachi A, Martin MA. 2007. Human immunodeficiency virus type 1 derivative with 7% simian immunodeficiency virus genetic content is able to establish infections in pig-tailed macaques. J. Virol. 81:11549–11552.
65. Lifson JD, Haigwood NL. 2012. Lessons in nonhuman primate models for AIDS vaccine research: from minefields to milestones. Cold Spring Harb. Perspect. Med. 2:a007310. doi:10.1101/cshperspect.a007310.
66. Shaw GM, Hunter E. 2012. HIV transmission. Cold Spring Harb. Perspect. Med. 2:a006965. doi:10.1101/cshperspect.a006965.

67. Swanstrom R, Coffin J. 2012. HIV-1 pathogenesis: the virus. Cold Spring Harb. Perspect. Med. 2:a007443. doi:10.1101/cshperspect.a007443.
68. Nishimura Y, Shingai M, Willey R, Sadjadpour R, Lee WR, Brown CR, Brenchley JM, Buckler-White A, Petros R, Eckhaus M, Hoffman V, Igarashi T, Martin MA. 2010. Generation of the pathogenic R5-tropic simian/human immunodeficiency virus $SHIV_{AD8}$ by serial passaging in rhesus macaques. J. Virol. 84:4769–4781.
69. Ren W, Mumbauer A, Gettie A, Seaman MS, Russell-Lodrigue K, Blanchard J, Westmoreland S, Cheng-Mayer C. 2013. Generation of lineage-related, mucosally transmissible subtype C R5 simian-human immunodeficiency viruses capable of AIDS development, induction of neurological disease, and coreceptor switching in rhesus macaques. J. Virol. 87:6137–6149.
70. Shingai M, Donau OK, Schmidt SD, Gautam R, Plishka RJ, Buckler-White A, Sadjadpour R, Lee WR, LaBranche CC, Montefiori DC, Mascola JR, Nishimura Y, Martin MA. 2012. Most rhesus macaques infected with the CCR5-tropic $SHIV_{AD8}$ generate cross-reactive antibodies that neutralize multiple HIV-1 strains. Proc. Natl. Acad. Sci. U. S. A. 109:19769–19774.
71. Shibata R, Kawamura M, Sakai H, Hayami M, Ishimoto A, Adachi A. 1991. Generation of a chimeric human and simian immunodeficiency virus infectious to monkey peripheral blood mononuclear cells. J. Virol. 65:3514–3520.
72. Kawamura M, Sakai H, Adachi A. 1994. Human immunodeficiency virus Vpx is required for the early phase of replication in peripheral blood mononuclear cells. Microbiol. Immunol. 38:871–878.
73. Gamble TR, Vajdos FF, Yoo S, Worthylake DK, Houseweart M, Sundquist WI, Hill CP. 1996. Crystal structure of human cyclophilin A bound to the amino-terminal domain of HIV-1 capsid. Cell 87:1285–1294.

Pathogens **2013**, *2*, 357-363; doi:10.3390/pathogens2020357

OPEN ACCESS

pathogens

ISSN 2076-0817

www.mdpi.com/journal/pathogens

Article

Presence of Viral Genome in Urine and Development of Hematuria and Pathological Changes in Kidneys in Common Marmoset (*Callithrix jacchus*) after Inoculation with Dengue Virus

Meng Ling Moi [1,†], Tsutomu Omatsu [1,2,†], Takanori Hirayama [1,3], Shinichiro Nakamura [4], Yuko Katakai [5], Tomoyuki Yoshida [6], Akatsuki Saito [6], Shigeru Tajima [1], Mikako Ito [1], Tomohiko Takasaki [1], Hirofumi Akari [6,*] and Ichiro Kurane [1,*]

1 National Institute of Infectious Diseases, 1-23-1 Toyama, Shinjuku-ku, Tokyo, 162-8640, Japan; E-Mails: sherry@nih.go.jp (M.L.M.); tomatsu@cc.tuat.ac.jp (T.O.); hirayama@jata.or.jp (T.H.); stajima@nih.go.jp (S.T.); mito0908@yahoo.co.jp (M.I.); takasaki@nih.go.jp (T.T.)

2 Tokyo University of Agriculture and Technology, 3-5-8 Fuchu, Tokyo, 183-8509, Japan

3 Japan Anti-tuberculosis Association, 3-1-24 Matsuyama, Kiyose, Tokyo, 204-8533, Japan

4 Shiga University of Medical Science, Seta Tsukinowa-cho, Otsu, Shiga, 520-2192, Japan; E-Mail: snakamur@belle.shiga-med.ac.jp

5 National Institute of Biomedical Innovation, 1 Hachimandai, Tsukuba, Ibaraki, 305-0843, Japan; E-Mail: katakai@primate.or.jp

6 Primate Research Institute, Kyoto University, Inuyama, Aichi, 484-8506, Japan; E-Mails: ytomoyuki@pri.kyoto-u.ac.jp (T.Y.); saito.akatsuki.6a@kyoto-u.ac.jp (A.S.)

† These authors contributed equally to the work.

* Authors to whom correspondence should be addressed; E-Mails: kurane@nih.go.jp (I.K.); akari@pri.kyoto-u.ac.jp (H.A.); Tel.: +81-03-5285-111 (I.K.); +81-0568-63-0440 (H.A.); Fax: +81-03-5285-1188 (I.K.); +81-0568-63-0459 (H.A.).

Received: 25 March 2013; in revised form: 27 April 2013 / Accepted: 8 May 2013 / Published: 13 May 2013

Abstract: Common marmosets (*Callithrix jacchus*) developed high levels of viremia, clinical signs including fever, weight loss, a decrease in activity and hematuria upon inoculation with dengue virus (DENV). Presence of DENV genome in urine samples and pathological changes in kidneys were examined in the present study. Levels of DENV genome were determined in 228 urine samples from 20 primary DENV-inoculated

marmosets and in 56 urine samples from four secondary DENV-inoculated marmosets. DENV genome was detected in 75% (15/20) of marmosets after primary DENV infection. No DENV genome was detected in urine samples from the marmosets with secondary infection with homologous DENV (0%, 0/4). Two marmosets demonstrated hematuria. Pathological analysis of the kidneys demonstrated non-suppressive interstitial nephritis with renal tubular regeneration. DENV antigen-positive cells were detected in kidneys. In human dengue virus infections, some patients present renal symptoms. The results indicate that marmosets recapitulate some aspects of the involvement of kidneys in human DENV infection, and suggest that marmosets are potentially useful for the studies of the pathogenesis of DENV infection, including kidneys.

Keywords: dengue virus; animal model; marmoset; urine; hematuria; kidney

1. Introduction

Dengue fever is a serious global health problem. In dengue fever patients, urine samples contain dengue virus (DENV) genomes and virus antigens were present in renal biopsies. However, the association between disease symptoms from appearance of DENV genome in urine, renal injury (occurrence rate of 2.9–13.3% of dengue patients) and haemolytic uraemic syndrome in the pathogenesis of dengue fever is unclear [1,2]. Poor outcome, including severe dengue and mortality, correlated with poor renal function [1]. To elucidate disease pathogenesis, it is important to establish an animal model that exhibits clinical signs which are comparable to those of human DENV infection. Marmosets develop high levels of viremia and demonstrate changes in biochemical and hematological parameters upon DENV inoculation [3,4]. In the present study, we constantly detected DENV genome in urine samples from DENV-inoculated marmosets. These marmosets also exhibited hematuria and pathological changes in the kidneys. The marmoset DENV infection model appears to recapitulate some aspects of DENV infection, and thus, offer the possibility of use in pathogenesis studies of DENV infection.

2. Results and Discussion

A total of 228 urine samples were obtained on days 1–14 from 20 marmosets after primary infection and 56 urine samples from four marmosets after homologous secondary infection (Table 1). DENV genome was detected in 18 of the 20 primary DENV-inoculated marmosets (Table 1, experiments 1–5). DENV genome was first detected three days after inoculation, and detected up to day 14. The levels of viral genome ranged from 3.8×10^3 to 8.4×10^7 copies/ml. The positive detection rates were 10% (8/82) on days 1–5, 20% (16/79) on days 6–10 and 27% (18/67) on days 11–14 after primary inoculation (Table 2). No DENV genome was detected in 56 urine samples (0%, 0/56) from 4 marmosets re-inoculated with the same serotype (Table 2, experiment 6, marmosets D2-2, D2-3, D2-4 and D2-5) on days 1–14 after inoculation. The detection rates in urine samples were 6% on day 3, the rates ranged from 17 to 31% (mean percentage = 22 ± 4%) on days 4–13, and 35% on day 14. In comparison to detection of viral genome in urine samples, DENV genome was detected on days 2–7 in serum samples (Table 2).

Table 1. Levels of dengue viral genome in urine samples from marmosets inoculated with dengue virus (DENV).

Animal ID	Virus strain	pfu/ dose	Dengue vRNA copy numbers (copies/ml) Days after inoculation 1	2	3	4	5	6	7	8	9	10	11	12	13	14
Primary inoculation																
Experiment 1																
D1-1	02-17/1	3.5×10^7	-	NT	NT	NT	7.5×10^4	-	NT	-	-	NT	-	-	-	-
D2-1	DHF0663	6.7×10^7	-	NT	NT	NT	3.8×10^3	2.5×10^4	7.0×10^4	4.0×10^4	5.0×10^4	3.7×10^4	6.5×10^4	4.2×10^3	1.0×10^4	-
D3-1	DSS1403	4.5×10^6	-	NT	NT	NT	-	-	NT	4.8×10^4	-	-	NT	8.5×10^4	-	-
D4-1	05-40/1	1.5×10^6	-	NT	NT	NT	-	-	NT	-	-	NT	-	-	-	-
Experiment-2																
D2-2	DHF0663	4.4×10^7	-	NT	8.3×10^4	-	-	-	2.9×10^5	1.8×10^5	-	-	-	8.1×10^4	-	-
D2-3			-	NT	-	7.3×10^4	-	7.1×10^4	1.5×10^5	-	4.8×10^5	-	-	-	-	-
D2-4		1.8×10^5	-	NT	-	-	1.4×10^5	-	-	-	-	-	-	-	-	2.0×10^5
D2-5			-	NT	-	-	-	-	-	-	-	-	-	-	-	-
Experiment-3																
D2-6	DHF0663	1.8×10^4	-	-	-	-	-	-	-	-	-	1.0×10^5	-	-	-	-
D2-7			-	-	-	-	-	-	-	-	-	-	-	-	-	8.5×10^4
D2-8		1.8×10^3	-	-	-	-	-	-	-	-	-	-	-	-	-	1.3×10^4
D2-9			-	-	-	-	-	-	-	-	-	-	1.9×10^4	-	-	-
Experiment-4																
D2-10	Jam/77/07	1.2×10^5	-	-	-	-	-	-	-	-	-	-	-	3.0×10^5	-	-
D2-11			-	-	-	6.7×10^3	-	-	-	-	-	-	-	-	-	4.2×10^5
D2-12	Mal/77/08	1.9×10^5	-	-	-	-	-	-	-	NT	-	5.9×10^6	1.7×10^5	-	7.8×10^5	-
D2-13			-	-	-	-	-	-	-	-	1.3×10^6	-	4.4×10^5	-	-	8.1×10^5
Experiment-5																
D2-14	DHF0663	6.7×10^7	-	-	-	*	*	*	*	*	*	*	*	*	*	*
D2-15			-	-	-	-	-	*	*	*	*	*	*	*	*	*
D2-16			-	-	-	-	-	-	*	*	*	*	*	*	*	*
D2-17			-	-	-	2.7×10^5	2.6×10^5	4.4×10^6	-	-	NT	8.4×10^7	5.9×10^7	-	1.9×10^7	8.2×10^6

- indicates viral RNA below limit of detection using RT-PCR, NT indicates not tested, * indicates that the marmosets were sacrificed and no samples were collected.

Table 2. Positive rates in the detection of DENV genome in urine samples on each of the 14 days following inoculation with DENV, in comparison with the previously reported data of serum samples [3].

Days after inoculation	Number of serum samples positive by RT-PCR (% positive, total tested)	
	Urine	Sera *
Day 1	0/20 (0)	NT †
Day 2	0/12 (0)	12/12
Day 3	1/16 (6)	7/8
Day 4	3/15 (20)	11/11
Day 5	4/19 (21)	4/5
Days 1–5	**8/82 (10)**	**34/36 (94)**
Day 6	3/18 (17)	NT
Day 7	3/14 (21)	11/18 (61)
Day 8	3/16 (19)	0/1 (0)
Day 9	3/16 (19)	NT
Day 10	4/15 (27)	0/4 (0)
Days 6–10	**16/79 (20)**	**11/23 (48)**
Day 11	5/16 (31)	NT
Day 12	4/17 (24)	NT
Day 13	3/17 (18)	NT
Day 14	6/17 (35)	0/17 (0)
Day 11–14	**18/67 (27)**	**0/17 (0)**
Total	**42/228 (18)**	**45/76 (59)**

* The DENV genome levels in serum samples were previously reported [3], † NT: indicates test not done.

In human dengue patients, DENV genome was detected in 30% (9/30) of urine samples as compared to 79% (34/43) in serum samples from days 1–5 after onset of disease, and 61% of urine samples as compared to serum samples (11%) on days 10–16 after onset of disease [5]. In marmosets, the rate of DENV genome-positive urine samples (10%, 8/82, Table 2) was lower as compared those of serum samples (94%, 34/36) on days 1–5 after DENV inoculation, and DENV genome was detected at a higher rate in urine samples (27%, 18/67) as compared to serum samples (0%, 0/17) on days 11–14 after infection (Table 2) [3]. Thus, the kinetics of viral genome clearance in urine and serum samples in marmosets were similar to those of human DENV patients. It is of interest that for both DENV patients and DENV-inoculated marmosets, infectious DENV was not detected in urine samples even when DENV genome was detected [5]. Limitations of our study include lack of data on the presence or absence of infectious virus in kidneys. Although DENV genome and viral antigen were present in kidneys, the antigens could represent reabsorbed immune complexes after clearance, and may suggest mechanisms other than viral replication in renal tissue, are involved in renal dysfunction during DENV infection.

Figure 1. Gross appearance of kidney and urine specimens of DENV inoculated marmosets. Urine samples for D1-1, D3-1 and D4-1 were pale yellow and clear (Figure 1A). Hematuria was detected in urine from DENV-2 inoculated marmoset D2-1 (indicated by a white arrow). Gross appearance of kidneys from marmosets inoculated with DENV-1 (marmoset D1-1, Figure 1B), DENV-2 (marmoset D2-1, Figure 1C), DENV-3 (marmoset D3-1, Figure 1D) and DENV-4 (marmoset D4-1, Figure 1E). The kidney from DENV-2 inoculated marmoset (D2-1) was swollen and fawn-colored (Figure 1C).

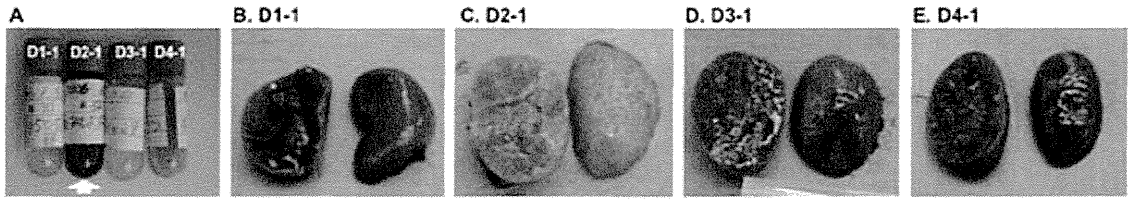

In comparison to the clear appearance of urine samples from DENV-1, DENV-3 and DENV-4 inoculated marmosets (D1-1, D3-1 and D4-1), marmoset D2-1 demonstrated apparent hematuria (Figure 1A). Microscopic hematuria was detected in marmoset D2-17 on days 5 and 8 after DENV inoculation but was not detected in other 7 marmosets tested (D2-6, D2-7, D2-8, D2-9, D2-14, D2-15, and D2-16) on days 1 to 14. Marmosets D1-1, D2-1 and D4-1 exhibited signs of ascitis formation (data not shown). Kidneys of both sides from marmoset D2-1 were swollen and fawn-colored (Figure 1C).

Figure 2. Histopathology associated with DENV-2 inoculation in marmosets. Severe non-suppressive interstitial nephritis with renal tubular degeneration was detected in kidney of DENV-2 inoculated marmoset (marmoset D2-1, Figure 2A). DENV-2 inoculated marmosets also exhibited moderate interstitial nephritis, and segmental glomerulosclerosis and renal tubular atrophy (D2-1, Figure 2B). Dengue viral antigen was detected in cells that morphologically correspond to lymphocytes and macrophages in the kidney from marmoset D2-17 (Figure 2C). Scale bar = 50 μm.

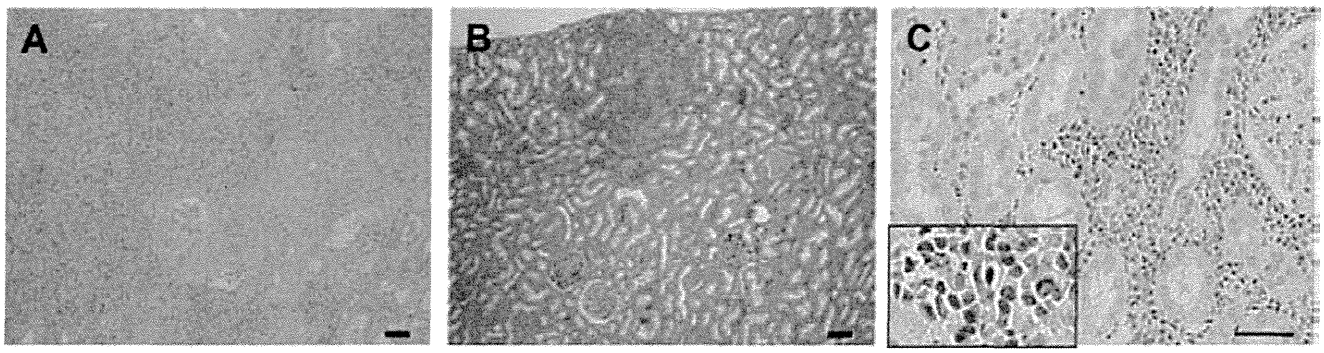

Upon histopathological examination, the kidney from marmoset D2-1 demonstrated significant renal lesions (Figure 2A,B). Despite the limited numbers of marmosets evaluated, levels of DENV genome in urine samples of two marmosets (D2-1 and D2-17) which demonstrated hematuria and significant renal lesions (mean virus titer = 3.7 log10 copies/ml) were higher as compared to urine samples from 18 marmosets which did not demonstrate hematuria (mean virus titer = 0.5 log10 copies/mL, $P < 0.01$; two-tailed Student's t-test). Mean genome positive days of urine samples for

marmosets D2-1 and D2-17 was 8.0 days as compared to 1.4 days for marmosets that did not demonstrate hematuria.

Renal dysfunction, occurs in 2.9–13.3% of human dengue patients, and is associated with disease severity [1,2]. Severity of renal dysfunction was also associated with higher percentages of severe dengue and mortality in humans. Although the number of marmosets used in the present study was limited, two DENV-inoculated marmosets (2/18, 11%) demonstrated clinical signs of the renal system. In addition to viremia and biochemical changes, development of these clinical signs in marmosets, suggests the feasibility of marmosets as an animal model to elucidate the pathogenesis of DENV infection, including the renal system.

3. Experimental Section

A total of 20 male common marmosets (*Callithrix jacchus*) were used in accordance with "Guides for animal experiments according to institutional guidelines (Approval no. 608011, 609014 and Approval no. 20-003, 21-013). The marmosets were inoculated subcutaneously in the back with either DENV-1, DENV-2, DENV-3 or DENV-4. Four marmosets (D2-2, D2-3, D2-4 and D2-5) were inoculated with the same serotype (DENV-2) at 33 weeks after primary inoculation [3]. DENV type 1 (DENV-1), 02-17/1 strain, DENV-2 DHF0663 strain (Accession no. AB189122), DENV-2 Jam/77/07 strain, DENV-2 Mal/77/08 strain, DENV-3 DSS1403 strain (Accession no. AB189125), and DENV-4 05-40/1 strain, were used for inoculation studies. Day 0 was defined as the day of virus inoculation. Urine samples were examined for gross hematuria for all 20 marmosets and a urine dipstick (Bayer Urine Dipstick, IN, USA) for marmosets D2-6, D2-7, D2-8, D2-9, D2-14, D2-15, D2-16 and D2-17). For histological analyses, paraffin-embedded tissues sections (4μm sections) were deparaffinized and stained with HE stain. For immunohistochemical analyses, sections were stained using HRP-conjugated marmoset polyclonal anti-DENV antibody. For viral RNA isolation, High Pure Viral RNA Kit (Roche Diagnostics) was used. To determine the levels of dengue viral RNA, each sample was assayed in a 25 μL reaction containing 5 μL of sample RNA, 0.9 μM of each forward and reverse DENV-serotype-specific primer, RT/RNAse Inhibitor Mix, 0.2 μM TaqMan DENV-serotype-specific probe, and TaqMan Universal Master Mix (Invitrogen). The thermal conditions were (1) reverse transcription at 48 °C for 30 minutes, (2) *Taq* polymerase activation at 95 °C for 10 minutes, (3) forty cycles of PCR consisting of denaturing at 95 °C for 15 seconds and annealing at 57 °C for 1 min [3]. RNA standards with RNA copies of 10^8 to 10^4 were used to quantify the dengue viral RNA. All TaqMan RT-PCR assays were performed in duplicate. Replicate variability threshold was set at 0.5, the RT-PCR detection limit of this study ranges from 3.1×10^2 to 4.4×10^4 copies/ ml for four DENV serotypes. Data analysis was done using Microsoft Excel and GraphPad Prism Statistical Package (Graphpad Software, CA, USA). Percentage of genome positive days was calculated using the formula (number of days with positive viral genome detection/ number of sampling days) × 100%.

4. Conclusions

Common marmosets demonstrate DENV genome in urine, hematuria and pathological changes of the kidneys upon DENV infection. The recapitulation of these clinical aspects of DENV infection,

including the involvement of kidneys, suggests the feasibility of the use of marmosets for studies on the pathogenesis of DENV infection.

Acknowledgments

This work was supported by grants from Research on Biological Resources and Animal Models for Drug Development (H19-Seibutsushigen-ippan-003) and Research on Emerging and Re-emerging Infectious Diseases (H20-shinkou-ippan-013, H21-shinkou-ippan-005, and H23-shinkou-ippan-010) from the Ministry of Health, Labour and Welfare, Japan. The funders had no role in study design, data collection and analysis, decision of submission for publication, or preparation of the manuscript.

Conflict of Interest

The authors declare no conflict of interest.

References

1. Kuo, M.C.; Lu, P.L.; Chang, J.M.; Lin, M.Y.; Tsai, J.J.; Chen, Y.H.; Chang, K.; Chen, H.C.; Hwang, S.J. Impact of renal failure on the outcome of dengue viral infection. *Clin. J. Am. Soc. Nephrol.* **2008**, *3*, 1350–1356.
2. Khalil, M.A.M.; Sarwar, S.; Chaudry, M.A.; Maqbool, B.; Khalil, Z.; Tan, J.; Yaqub, S.; Hussain, S.A. Acute kidney injury in dengue virus infection. *Clin. Kid. J.* **2012**, *5*, 390–394.
3. Omatsu, T.; Moi, M.L.; Hirayama, T.; Takasaki, T.; Nakamura, S.; Tajima, S.; Ito, M.; Yoshida, T.; Saito, A.; Katakai, Y.; Akari, H.; Kurane, I. Common marmoset (Callithrix jacchus) as a primate model of dengue virus infection: Development of high levels of viraemia and demonstration of protective immunity. *J. Gen. Virol.* **2011**, *92*, 2272–2280.
4. Omatsu, T.; Moi, M.L.; Takasaki, T.; Nakamura, S.; Katakai, Y.; Tajima, S.; Ito, M.; Yoshida, T.; Saito, A.; Akari, H.; Kurane, I. Changes in hematological and serum biochemical parameters in common marmosets (Callithrix jacchus) after inoculation with dengue virus. *J. Med. Primatol.* **2012**, *41*, 289–296.
5. Hirayama, T.; Mizuno, Y.; Takeshita, N.; Kotaki, A.; Tajima, S.; Omatsu, T.; Sano, K.; Kurane, I.; Takasaki, T. Detection of dengue virus genome in urine by real-time reverse transcriptase PCR: A laboratory diagnostic method useful after disappearance of the genome in serum. *J. Clin. Microbiol.* **2012**, *50*, 2047–2052.

JVI
Journals.ASM.org

Natural Single-Nucleotide Polymorphisms in the 3′ Region of the HIV-1 *pol* Gene Modulate Viral Replication Ability

Masako Nomaguchi,[a] Ariko Miyake,[a] Naoya Doi,[a] Sachi Fujiwara,[a] Yasuyuki Miyazaki,[a] Yasuko Tsunetsugu-Yokota,[b] Masaru Yokoyama,[c] Hironori Sato,[c] Takao Masuda,[d] Akio Adachi[a]

Department of Microbiology, Institute of Health Biosciences, The University of Tokushima Graduate School, Tokushima, Japan[a]; Department of Immunology, National Institute of Infectious Diseases, Tokyo, Japan[b]; Laboratory of Viral Genomics, Pathogen Genomics Center, National Institute of Infectious Diseases, Tokyo, Japan[c]; Department of Immunotherapeutics, Graduate School of Medicine and Dentistry, Tokyo Medical and Dental University, Tokyo, Japan[d]

ABSTRACT

We previously showed that prototype macaque-tropic human immunodeficiency virus type 1 (HIV-1) acquired nonsynonymous growth-enhancing mutations within a narrow genomic region during the adaptation process in macaque cells. These adaptive mutations were clustered in the 3′ region of the *pol* gene, encoding a small portion of the C-terminal domain of integrase (IN). Mutations in HIV-1 IN have been reported to have pleiotropic effects on both the early and late phases in viral replication. *cis*-acting functions in the IN-coding sequence for viral gene expression have also been reported. We here demonstrated that the adaptive mutations promoted viral growth by increasing virion production with no positive effects on the early replication phase. Synonymous codon alterations in one of the adaptive mutations influenced virion production levels, which suggested nucleotide-dependent regulation. Indeed, when the single-nucleotide natural polymorphisms observed in the 3′ regions of 196 HIV-1/simian immunodeficiency virus (SIVcpz) *pol* genes (nucleotides [nt] 4895 to 4929 for HIV-1 NL4-3) were introduced into macaque- and human-tropic HIV-1 clones, more than half exhibited altered replication potentials. Moreover, single-nucleotide mutations caused parallel increases or decreases in the expression levels of viral late proteins and viral replication potentials. We also showed that the overall expression profiles of viral mRNAs were markedly changed by single-nucleotide mutations. These results demonstrate that the 3′ region of the HIV-1 *pol* gene (nt 4895 to 4929) can alter viral replication potential by modulating the expression pattern of viral mRNAs in a nucleotide-dependent manner.

IMPORTANCE

Viruses have the plasticity to adapt themselves under various constraints. HIV-1 can mutate and evolve in growth-restrictive cells by acquiring adaptive changes in its genome. We have previously identified some growth-enhancing mutations in a narrow region of the IN-coding sequence, in which a number of *cis*-acting elements are located. We now focus on the virological significance of this *pol* gene region and the mechanistic basis underlying its effects on viral replication. We have found several naturally occurring synonymous mutations within this region that alter viral replication potentials. The effects caused by these natural single-nucleotide polymorphisms are linked to the definite expression patterns of viral mRNAs. We show here that the nucleotide sequence of the *pol* gene (nucleotides 4895 to 4929 for HIV-1 NL4-3) plays an important role in HIV-1 replication by modulating viral gene expression.

The gene expression process of human immunodeficiency virus type 1 (HIV-1) (transcription, capping, polyadenylation, splicing, nuclear export, and translation) is highly coordinated and regulated by interactions between host/viral proteins and *cis*-acting elements located within the viral genome (1, 2). During this process, more than 40 mRNA species with nine viral genes are generated by alternative splicing (3, 4). These mRNA species are divided into three major groups: ~9-kb mRNAs (unspliced form) encoding Gag and Gag-Pol proteins, ~4-kb mRNAs (singly spliced form) encoding Vif, Vpr, Vpu, and Env proteins, and ~1.8-kb mRNAs (completely spliced form) encoding Tat, Rev, and Nef proteins. In the early phase of HIV-1 gene expression, ~1.8-kb mRNA species are transported to the cytoplasm and translated to synthesize Tat, Rev, and Nef proteins. Tat, along with some host factors, *trans*-activates HIV-1 transcription (5, 6). Rev facilitates the nuclear export of ~4-kb and ~9-kb HIV-1 mRNAs, and their encoded proteins are subsequently produced (7, 8). Alterations in the tightly regulated process of HIV-1 gene expression can affect viral replication (3, 4, 9–11).

HIV-1 integrase (IN) is generated from a Gag-Pol precursor and mediates integration, a hallmark of retroviruses. HIV-1 IN is involved not only in integration but also in reverse transcription, viral DNA nuclear import, and virion assembly/production (12–19). The deletion or C-terminal truncation of HIV-1 IN has been shown to reduce virion production in producer cells (20, 21). Although mutations in IN have negative effects on virion production, they also affect the early phase of viral replication (15, 22). Different amino acid substitutions at the same sites often have diverse effects on viral replication potential (13, 15, 23, 24). Furthermore, a number of splicing sites and *cis*-acting elements have been identified in the IN-coding sequence (3, 4, 25–30). There-

Received 9 July 2013 Accepted 20 January 2014
Published ahead of print 29 January 2014
Editor: W. I. Sundquist
Address correspondence to Akio Adachi, adachi@basic.med.tokushima-u.ac.jp.

doi:10.1128/JVI.01859-13

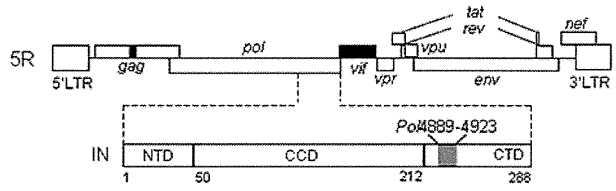

Amino acid position in IN	5R		Adapted clones	
	Amino acid	Codon	Amino acid	Codon
222	N	AAT	K	AAA
223	F	TTT	Y	TAT
229	D	GAC	E	GAA
234	V	GTT	I	ATT

FIG 1 Growth-enhancing mutations identified in the 3′ region of the *pol* gene. The genome structure of 5R (34) (GenBank accession no. AB266485) is schematically depicted. Black areas show the sequence derived from SIVmac239 (56) (GenBank accession no. M33262). The *pol* region encoding IN and the IN domain structure are indicated. The gray area represents a region in the *pol* gene (nt 4889 to 4923) designated *Pol*4889-4923, in which adaptive mutations are located. NTD, N-terminal domain; CCD, catalytic core domain; CTD, C-terminal domain. Details of the adaptive mutations found in the *Pol*4889-4923 region are shown at the bottom.

fore, mutations in the IN-coding sequence can change the nucleotide sequence important for viral replication as well as the protein-coding sequence associated with IN activity. The replication-defective mutant IN E246K represents a good example. It showed a processing defect in Gag, and its virion production level was markedly reduced (15). The E246K mutation, which is located within splicing site D2 and affects viral RNA splicing, was shown to result in the loss of viral infectivity (31). Thus, *cis*-acting functions in the IN-coding sequence must be considered to delineate its possible roles in viral replication.

In a previous virus adaptation study, we demonstrated that growth-enhanced viruses, which emerged following a long-term culture of cells infected with macaque-tropic HIV-1 NL-DT5R (5R) or NL-DT562 (562), frequently and reproducibly acquired mutations in the 3′ region of the *pol* gene (nucleotides [nt] 4889 to 4923 for 5R [Fig. 1] and nt 4895 to 4929 for the standard HIV-1 NL4-3), which encodes a small portion of the IN C-terminal domain (CTD) (32). Four adaptive mutations (N222K, F223Y, D229E, and V234I) in the region were identified in our repeated virus adaptation experiments and were responsible for viral growth enhancements (32). In this study, we aimed to elucidate how mutations in the 3′ region of the *pol* gene promoted viral replication and what the virological significance of this region was. The four mutations mentioned above were found to augment virus replication potential by increasing infectious virion production without any effects on the early replication phase. The CTD has been reported to be the least conserved sequence of the three domains in IN (15, 17, 19), with the 234th amino acid in IN being polymorphic (33). Codon alterations in V234I from ATT to ATC and ATA influenced virion production, which indicated regulation by a single-nucleotide change. An investigation of the sequences in the 3′ region of the *pol* gene in 196 HIV-1/simian immunodeficiency virus (SIVcpz) genomes (HIV sequence compendium 2011, Los Alamos National Laboratory, NM, USA) revealed that natural variants carried ATT or ATC at amino acid position 234. Based on these findings, single-nucleotide natural variations in the 3′ region of the *pol* gene (nt 4895 to 4929 for NL4-3) were introduced into macaque- and human-tropic HIV-1 clones. We identified several natural variations that alter virion production/replication efficiency. The observed effects of single-nucleotide variations were attributed to an increase or decrease in the expression levels of viral late proteins (Gag, Gag-Pol, Vpu, and Env), whereas early proteins (Nef and Rev) were invariably expressed. Moreover, single-nucleotide variations caused changes in the viral mRNA expression pattern. Taken together, our results showed that the nucleotide sequence of the 3′ region of the HIV-1 *pol* gene (nt 4895 to 4929 for NL4-3) play an important role in viral replication by modulating viral gene expression.

MATERIALS AND METHODS

Plasmid DNAs. The proviral clones pNL-DT5R (34) and pNL4-3 (35) were used as parental clones in the present study. Proviral clones carrying each mutation in the 3′ region of the *pol* gene were constructed with the QuikChange site-directed mutagenesis kit (Agilent Technologies Inc., Santa Clara, CA). Proviral *env*-deficient clones were constructed by deleting the NdeI (nt 6584)-NheI (nt 7435) fragment of pNL-DT5R. Reporter clones were constructed by introducing the luciferase gene into the *nef* gene of *env*-deficient proviral clones as described previously (36). A long terminal repeat (LTR)-driven luciferase reporter clone (5RLTR-Luc) was constructed by replacing the AatII (5′end of the proviral genome)-NcoI (5′end of the luciferase gene in the *nef* gene) fragment of the pNL-DT5R luciferase reporter clone with the LTR region (nt 1 to 789) of pNL-DT5R. A proviral *gag/gag-pol* frameshift clone (gtg-Spe) was constructed by cutting the V234gtg clone with SpeI (nt 1501) within the *gag* capsid and inserting four nucleotides with T4 DNA polymerase.

Cells. Human kidney 293T cells were cultured in minimal essential medium (MEM) supplemented with 10% heat-inactivated fetal bovine serum (hiFBS). Human lymphocyte M8166 cells were cultured in RPMI 1640 supplemented with 10% hiFBS. Human lymphocyte MT4/CCR5 cells (MT4 cells stably expressing CCR5) were maintained in RPMI 1640 containing 10% hiFBS and 200 μg/ml of hygromycin B (Sigma-Aldrich Co., St. Louis, MO).

Analysis of virus growth kinetics. Virus stocks were prepared from 293T cells transfected with proviral clones as previously described (34, 35). Virion-associated reverse transcriptase (RT) activity was measured as previously described (37). M8166 and MT4/CCR5 cells (10^5) were infected with equal amounts of NL-DT5R and its derivative viruses (35 RT units and 5×10^5 RT units for M8166 and MT4/CCR5 cells, respectively), as previously described (38, 39). Equal amounts (10^5 RT units) of HIV-1 NL4-3 and its derivative viruses were inoculated into MT4/CCR5 cells (10^5). Virus replication was monitored by RT activity released into the culture supernatants.

Analysis of single-cycle viral infectivity. Vesicular stomatitis virus G protein (VSV-G)-pseudotyped viruses were prepared from 293T cells cotransfected with an *env*-deficient luciferase reporter clone and pCMV-G (40) at a molar ratio of 1:1. Virus amounts on day 2 posttransfection were measured with an HIV-1 p24 antigen enzyme-linked immunosorbent assay (ELISA) kit (ZeptoMetrix Corporation, Buffalo, NY). M8166 cells (10^5) were infected with equal amounts of pseudotyped viruses (30 pg of p24), and cells were lysed on day 1 postinfection for luciferase assays (Promega Corporation, Madison, WI).

Analysis of viral cDNA synthesis. DNase I-treated pseudoviruses (150 pg of p24) were inoculated into M8166 cells (5×10^5), and total DNA was extracted on day 1 postinfection using the DNeasy blood and tissue kit (Qiagen GmbH, Hilden, Germany). Quantitative analyses of viral cDNA products using real-time quantitative PCR (ABI7500; Life Technologies Corporation, Carlsbad, CA) were performed as previously described (14).

Analysis of virion production. M8166 cells (10^6) were cotransfected with equal amounts of *env*-deficient proviral clones (1 μg) and the pGL3

luciferase reporter vector (Promega Corporation) (1 μg) using the Amaxa human T cell Nucleofector kit (Lonza Ltd., Basel, Switzerland) with Nucleofector II (Lonza Ltd.). Culture supernatants were collected on day 2 posttransfection, and virion production was measured using the HIV-1 p24 antigen ELISA kit (ZeptoMetrix Corporation). Cell lysates were prepared with 1× CCLR buffer (Promega Corporation) and subjected to luciferase assays (Promega Corporation). The luciferase activity in cell lysates was used to normalize the transfection efficiency.

Analysis of viral protein expression. 293T cells for Western blot analysis were transfected with equal amounts of proviral clones by using Lipofectamine 2000 (Life Technologies Corporation) in the absence or presence of 2 μM saquinavir (SQV) (Sigma-Aldrich Co.). On day 1 posttransfection, cells were lysed in 1× TNE buffer (10 mM Tris-HCl [pH 8.0], 1% Nonidet P-40, 150 mM NaCl, 1 mM EDTA [pH 8.0], and 1% protease inhibitor cocktail [Sigma-Aldrich Co.]). The total protein amounts in the cell lysates were measured with the DC protein assay (Bio-Rad Laboratories Inc., Hercules, CA), and equal amounts were loaded onto Mini-Protean TGX gels (Bio-Rad Laboratories Inc.) for electrophoresis (0.5 μg for the anti-gp160 antibody, 1 μg for the anti-Vpu antibody, 2 μg for the anti-p24, anti-Nef, or anti-β-actin antibody, 5 μg for the anti-Rev antibody, and 20 μg for the anti-RT antibody). Following blotting onto Immobilon-P transfer membranes (Merck KGaA, Darmstadt, Germany), the membranes were treated with the anti-β-actin clone AC-15 (Sigma-Aldrich Co.), anti-HIV-1 p24 (183-H12-5C) (catalog number 3537; NIH Research and References Reagent Program), anti-HIV-1 RT (MP Biomedicals, Santa Ana, CA), HIV-1 NL4-3 Vpu antiserum (catalog number 969; NIH Research and References Reagent Program), anti-HIV-1 gp160 (ADP409; Immuno Ltd./the MRC AIDS Directed Programme Reagent Project), anti-Rev (ab25871; Abcam PLC, Cambridge, England), or anti-HIV-1 Nef (Advanced Biotechnologies Inc., Columbia, MD) antibody and visualized with the Amersham ECL Plus Western blotting detection system (GE Healthcare UK Ltd., Buckinghamshire, England). A GS-800 calibrated densitometer and Quantity One software (Bio-Rad Laboratories Inc.) were used to quantify signal intensities. To monitor the expression levels of viral proteins, 293T cells were transfected with proviral clones by using Lipofectamine 2000 (Life Technologies Corporation), and on day 2 posttransfection, samples were prepared as described above. The amounts of cell-associated Gag-p24 and Pol-RT were measured using the HIV-1 p24 antigen ELISA kit (ZeptoMetrix Corporation) and RT capture ELISA kit (ImmunoDX, LLC, Woburn, MA), respectively. To monitor Tat activity, 293T cells were cotransfected with proviral clones (0.2 μg) and the 5RLTR-Luc clone (0.05 μg) by using Lipofectamine 2000 (Life Technologies Corporation). Cells were lysed with 1× CCLR buffer (Promega Corporation) on day 1 posttransfection for luciferase assays (Promega Corporation). 293T cells for the interference experiments were transfected with an appropriate amount of proviral clones (5R and its derivatives) by using Lipofectamine 2000 (Life Technologies Corporation). Cells were lysed with 1× TNE buffer on day 1 posttransfection, and the amount of Gag-p24 in cell lysates was measured using the HIV-1 p24 antigen ELISA kit (ZeptoMetrix Corporation).

Northern blot analysis. 293T cells were transfected with equal amounts of proviral clones by using Lipofectamine 2000 (Life Technologies Corporation), and total RNA was extracted at 10 to 20 h posttransfection using the RNeasy Plus Minikit (Qiagen GmbH). Poly(A)$^+$ RNA was isolated with the Oligotex-dT30 Super mRNA purification kit (TaKaRa Bio Inc., Otsu, Japan) and then treated with DNase I (TaKaRa Bio Inc.). Equal amounts of RNA samples were loaded on a glyoxal denatured 1% agarose gel prepared with NorthernMax-Gly 10× Gel Prep/running buffer (Life Technologies Corporation), electrophoresed, and blotted onto a positively charged nylon membrane (Roche Diagnostics GmbH, Mannheim, Germany). The digoxigenin (DIG)-labeled universal probe (U probe) to detect all HIV-1 mRNA species was prepared by using a PCR DIG probe synthesis kit (Roche Diagnostics GmbH.) with pNL4-3 as a template and primers 5′-GAGGATTGTGGAACTTCTGG-3′ and 5′-CTTTGGGAGTGAATTAGCCC-3′. The DIG-labeled Rev-responsive element (RRE) probe, vif probe, and vpr probe were synthesized using templates and primer pairs as follows: RRE probe, pNL4-3, forward primer 5′-CCATTAGGAGTAGCACCCAC-3′, and reverse primer 5′-GTTCCAGAGATTTATTACTCC-3′; vif probe, pNL-DT5R, forward primer 5′-ATGGAGGAGGAAAAGAGGTGG-3′, and reverse primer 5′-CTGCATAAGTACTGAGCCAC-3′; and vpr probe, pNL4-3, forward primer 5′-ATGGAACAAGCCCCAGAAG-3′, and reverse primer 5′-GCAGAATTCTTATTATGGCTTCC-3′. The membrane was hybridized with the DIG-labeled probe in DIG Easy Hyb (Roche Diagnostics GmbH), and visualized with the DIG High Prime DNA labeling and detection starter kit II (Roche Diagnostics GmbH). To monitor and normalize loading amounts of RNAs, membranes were hybridized with the random-prime DIG-labeled GAPDH (glyceraldehyde-3-phosphate dehydrogenase) probe prepared with the DIG High Prime DNA labeling and detection starter kit II (Roche Diagnostics GmbH) and visualized as described above.

RESULTS

Growth-enhancing adaptive mutations increase virion production but have no effects on the early phase of viral replication. We previously obtained adapted viruses with enhanced growth potential from long-term cultures of macaque cells infected with macaque-tropic HIV-1 5R (34) or its R5-tropic version 562 (41). While proviral clones generated from adapted viruses contained a number of mutations in scattered regions of the viral genomes, only mutations in *pol*-IN or *env*-Gp120 were found to contribute to viral growth enhancement (32). In this study, we investigated the mechanistic basis for acceleration of viral replication by the adaptive mutations in the IN-coding sequence. As indicated in Fig. 1, four mutations (N222K, F223Y, D229E, and V234I in the 3′ region of the *pol* gene designated *Pol*4889-4923) were previously shown to enhance viral growth in macaque cells (32). The introduction of both N222K and V234I into human-tropic HIV-1 NL4-3 had a growth-enhancing effect in human cells similar to that observed for 5R (32). We first studied the effect of the adaptive mutations in the *Pol*4889-4923 region on viral replication in M8166 cells. As shown in Fig. 2A, all mutants grew more efficiently than the parental 5R virus. To examine the early replication phase, single-cycle viral infectivity was determined by infection with VSV-G-pseudotyped viruses containing a luciferase gene in the *nef* gene. All mutant clones exhibited infectivity similar to that of 5R (Fig. 2B). Furthermore, the four mutations did not have positive effects on viral cDNA synthesis, as measured by real-time quantitative PCR (Fig. 2C). All four growth-enhancing mutations resulted in an increase in virion production in transfected M8166 cells (Fig. 2D). An enhancement in virion production was consistently observed for pseudotyped and proviral clones in transfected 293T cells (data not shown). These results showed that the acceleration of viral replication by the adaptive mutations in the *Pol*4889-4923 region could be attributed to the increase in infectious virion production in producer cells.

Amino acid substitutions caused by the adaptive mutations may not be responsible for the enhancement in virion production/replication ability. All growth-enhancing mutations in the *Pol*4889-4923 region were nonsynonymous changes (Fig. 1). To determine whether altered amino acids were critical for the enhancement in virion production/replication efficiency, each amino acid at the four sites (N222, F223, D229, and V234) was replaced by various amino acids with different sizes and chemical properties (detailed in Table 1). The effects of amino acid substitutions at these positions on virion production and viral replica-

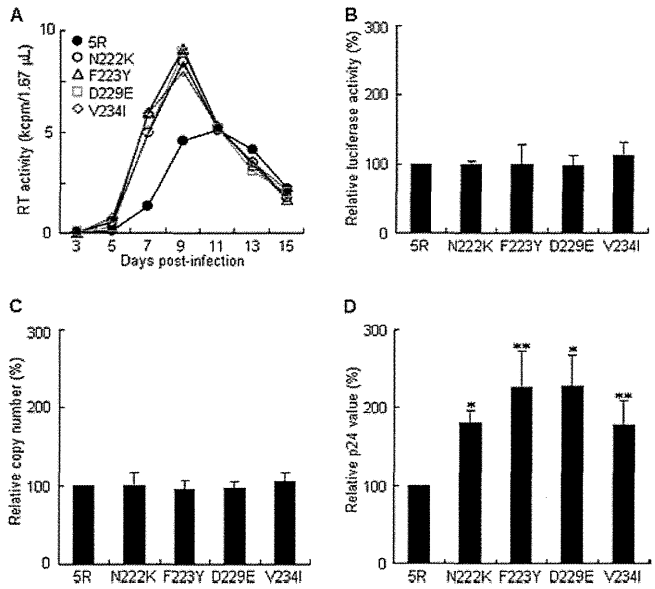

FIG 2 Effect of the adaptive mutations in the *Pol*4889-4923 region on different stages of virus replication in M8166 cells. (A) Replication kinetics. Input viruses were prepared from 293T cells transfected with the indicated proviral clones, and equal amounts were inoculated into M8166 cells. Virus replication was monitored by RT activity released into the culture supernatants. Representative data from at least three independent experiments are shown. (B) Single-cycle viral infectivity. VSV-G-pseudotyped viruses were prepared from 293T cells transfected with the indicated clones, and equal amounts were inoculated into M8166 cells. Cell lysates were prepared on day 1 postinfection and subjected to luciferase assays. Infectivity is presented as luciferase activity relative to that exhibited by 5R. Mean values from three independent experiments are shown with the standard deviations (SD). (C) Viral cDNA synthesis. VSV-G-pseudotyped viruses were prepared from 293T cells transfected with the indicated clones, DNase I treated, and inoculated into M8166 cells. Total DNA was extracted from infected cells on day 1 postinfection and subjected to real-time quantitative PCR analyses with a primer pair specific for the late form (R/gag) of viral cDNA. The DNA copy number relative to that of 5R is presented. Mean values ± SD from three independent experiments are shown. (D) Virion production. M8166 cells were cotransfected with the indicated *env*-deficient proviral clones and a luciferase reporter vector (pGL3) by using a Nucleofector. Virion production on day 2 posttransfection was measured by the amount of Gag-p24 in the culture supernatants. The amount of p24 was normalized by luciferase activity in cell lysates. The amount of p24 relative to that produced by 5R is presented. Mean values ± SD from four independent experiments are shown. Significance relative to 5R as calculated by the Student *t* test is shown (*, $P < 0.01$; **, $P < 0.02$).

tion (Fig. 3) were determined as described above. As shown in Fig. 3A, for N222, the virion production level relative to that of 5R was enhanced by the substitution with Ala (A) and Gly (G) as well as the growth-enhancing adaptive mutation Lys (K) but was decreased by the substitution with Phe (F) and Tyr (Y). The increase and decrease in virion production caused by these amino acid substitutions at N222 positively correlated with viral growth potential (Fig. 3A). For F223 (Fig. 3B), all mutant clones carrying Ala (A), Glu (E), Gly (G), His (H), Lys (K), and Ser (S) in addition to the adaptive mutation Tyr (Y) produced more virions than 5R, whereas only F223Y augmented viral replication efficiency. To study the cause of this apparent discrepancy, we compared the effects of F223Y and F223A/E/H/S on the early replication phase (Fig. 4). While F223Y showed levels of single-cycle viral infectivity and viral cDNA synthesis (late and integrated forms) similar to those for 5R, marked differences were observed in the behaviors of the other mutants. The virus infectivity of F223H was approximately 30% to that of 5R, and the infectivity of F223A/E/S was undetectable (Fig. 4A). A reduction in viral cDNA levels was also observed for F223A/E/H/S (Fig. 4B and C). These results indicate that the F223 residue is essential for the function of IN in the early replication phase. For D229 (Fig. 3C), virion production/replication ability was enhanced only by the adaptive mutation Glu (E), and the other mutants carrying D229A/G/T/W had reduced virion production/replication potential. For V234 (Fig. 3D), the Gly (G) substitution as well as the adaptive mutation Ile (I) augmented virion production/replication capability, but V234A/W decreased these. Because mutants D229K and V234E produced virions at the 5R level upon transfection (Fig. 3C and D), they are most likely to be defective for the early replication phase like the F223 mutants (Fig. 3B and 4). The results in Fig. 3 clarify the clear correlation between virion production and viral growth potential, except for the F223 mutants and the D229K/V234E mutants. However, increases or decreases in virion production were not dependent on altered amino acid sizes or chemical properties (Table 1). For example, virion production levels were enhanced by any altered amino acids tested at F223, and V234G and V234A increased and decreased virion production levels, respectively, despite their similar amino acid properties. Therefore, these results indicate that amino acid residues may not be a determinant for virion production.

Synonymous codon changes in V234I alter virion production/replication ability. Although no clear relationship was observed between the amino acids in the *Pol*4889-4923 region and increase in virion production (Table 1), virion production levels were markedly affected by the substitutions with different amino acids (Fig. 3). Since nucleotide mutations in the IN-coding sequence can induce viral phenotypic changes as described above, we speculated about the possible involvement of codon/nucleotide sequences in virion production enhancements. Thus, proviral clones carrying different codons for growth-enhancing mutations were constructed (N222K-2, F223Y-2, D229E-2, V234I-2, and V234I-3), and their growth potentials were compared to those of 5R and parental clones with each adaptive mutation. As shown in Fig. 5A, the growth of codon-altered viral clones (N222K-2, F223Y-2, and D229E-2) was more efficient than that of 5R, as observed for N222K, F223Y, and D229E. A fluctuation in viral replication potential among the V234I codon variants was noted: the growth abilities of V234I and V234I-3 were higher than that of 5R, but that of for V234I-2 was slightly impeded (Fig. 5A). While the single-cycle early infectivities of 5R and these codon variants were similar (Fig. 5B), their virion production levels varied in parallel with their replication potentials (Fig. 5A and C). Only V234I-2 exhibited a virion production level similar to that of 5R, and the other codon-altered mutants showed an enhanced level of virion production. The results for the V234I codon variants demonstrate the alteration in virion production levels in a nucleotide sequence-dependent manner, resulting in the modulation of viral replication ability.

Virion production levels of V234I codon variants correlate with Gag and Gag-Pol expression levels in producer cells. Synonymous codon changes in Ile (I) at amino acid position 234 in *pol*-IN caused an alteration in infectious virion production levels (Fig. 5C). We assumed that at least Gag and Gag-Pol expression levels, prerequisites for virion formation, correlatively varied with the amount of progeny virions. It has also been shown that cell-

TABLE 1 Characteristics of viral clones carrying various mutations in the 3′ region of the *pol* gene

Amino acid position in IN	Viral clone name	Amino acid	Codon	Size of amino acid	Chemical property(ies) of amino acid	Early replication[a]	Virion production[a]	Growth[b]
222	5R	N	AAT	Medium-small	Neutral, hydrophilic	++	++	++
	N222K[c]	K	AAA	Medium-large	Basic	++	+++	+++
	N222K-2	K	AAG	Medium-large	Basic	++	+++	+++
	N222A	A	GCT	Small	Aliphatic, hydrophobic	ND[d]	+++	+++
	N222G	G	GGT	Small	Aliphatic, hydrophobic	ND	+++	+++
	N222F	F	TTC	Large	Aromatic, hydrophobic	ND	+	−
	N222Y	Y	TAT	Large	Aromatic	ND	++	+
223	5R	F	TTT	Large	Aromatic, hydrophobic	++	++	++
	F223Y[c]	Y	TAT	Large	Aromatic	++	+++	+++
	F223Y-2	Y	TAC	Large	Aromatic	++	+++	+++
	F223H	H	CAT	Large	Basic	+	+++	+
	F223G	G	GGT	Small	Aliphatic, hydrophobic	ND	+++	−
	F223A	A	GCT	Small	Aliphatic, hydrophobic	−	+++	−
	F223S	S	TCT	Small	Neutral, hydrophilic	−	+++	−
	F223E	E	GAA	Medium-large	Acidic	−	+++	−
	F223K	K	AAA	Medium-large	Basic	ND	+++	−
229	5R	D	GAC	Medium-small	Acidic	++	++	++
	D229E[c]	E	GAA	Medium-large	Acidic	++	+++	+++
	D229E-2	E	GAG	Medium-large	Acidic	++	+++	+++
	D229K	K	AAA	Medium-large	Basic	ND	++	+
	D229A	A	GCC	Small	Aliphatic, hydrophobic	ND	+	−
	D229G	G	GGC	Small	Aliphatic, hydrophobic	ND	+	+
	D229T	T	ACC	Medium-small	Neutral, hydrophilic	ND	−	−
	D229W	W	TGG	Large	Aromatic, hydrophobic	ND	−	−
234	5R	V	GTT	Medium-small	Aliphatic, hydrophobic	++	++	++
	V234I[c]	I	ATT	Medium-small	Aliphatic, hydrophobic	++	+++	+++
	V234I-2	I	ATC	Medium-small	Aliphatic, hydrophobic	++	++	+
	V234I-3	I	ATA	Medium-small	Aliphatic, hydrophobic	++	+++	+++
	V234G	G	GGT	Small	Aliphatic, hydrophobic	ND	+++	+++
	V234A	A	GCT	Small	Aliphatic, hydrophobic	ND	+	+
	V234E	E	GAA	Medium-large	Acidic	ND	++	+
	V234W	W	TGG	Large	Aromatic, hydrophobic	ND	+	+

[a] +++, >150% of 5R activity; ++, >70 to 150% of 5R activity; +, 10 to 70% of 5R activity; −, <10% of 5R activity. Data were obtained in M8166 cells.

[b] +++, replication peaked earlier or virus production levels on the peak day were higher than those of 5R; ++, replication kinetics were similar to those of 5R; +, replication peaked later or virus production levels on the peak day were lower than those of 5R; −, replication was not detected during the observation period. Data were obtained in M8166 cells.

[c] Adaptive (growth-enhancing) mutation.

[d] ND, not done.

associated Gag was decreased for *pol*-IN deletion mutant viruses defective in virion production (20). To determine intracellular Gag and Gag-Pol expression levels, the proviral clones of 5R and V234I codon variants were transfected into 293T cells in the presence or absence of the HIV-1 protease inhibitor SQV. First, intracellular Gag-p24 and Pol-RT in the absence of SQV were measured by ELISA. While V234I and V234I-3, with improved virion production potential, expressed higher levels of Gag-p24 and Pol-RT than 5R, V234I-2 and 5R generated similar amounts (Fig. 6A). We then examined the intracellular expression patterns of Gag and Gag-Pol by Western blotting analyses. The expression profiles of $Pr55^{Gag}$/p24 and $Pr160^{Gag\text{-}Pol}$/p66/p51 for 5R and V234I codon variants were similar in the absence of SQV, which strongly suggested the absence of an effect of V234I mutations on viral protein processing [Fig. 6B SQV(−)]. The expression levels of Gag/Gag-Pol-related proteins were higher for V234I and V234I-3 than for 5R [Fig. 6B and C, SQV(−)]. In contrast, V234I-2 appeared to express slightly lower levels of these viral proteins than 5R [Fig. 6B and C, SQV(−)]. This small decrease in Gag/Gag-Pol expression levels may be consistent with the similar difference observed for the viral replication kinetics of 5R and V234I-2 (Fig. 5A). The variations in $Pr55^{Gag}$ and $Pr160^{Gag\text{-}Pol}$ expression levels in the presence of SQV appeared to be smaller than those obtained by Western blotting analyses [Fig. 6B and C, SQV(+)]. This may have been due to the weak recognition of $Pr55^{Gag}$ and $Pr160^{Gag\text{-}Pol}$ by the antibodies used. The results described above show that the alteration in the virion production/replication potential of V234I codon variants is in parallel with the increase or decrease in Gag/Gag-Pol expression levels.

Viral replication capability can be altered by natural variations in the sequences of the 3′ region of the HIV-1 *pol* gene. As observed for V234I codon variants, single-nucleotide changes resulted in alterations in virion production/replication potential through the modulation of Gag/Gag-Pol expression levels, which indicated the importance of the nucleotide sequence in the *Pol*4889-4923 region (Fig. 5 and 6). Recent studies revealed that a

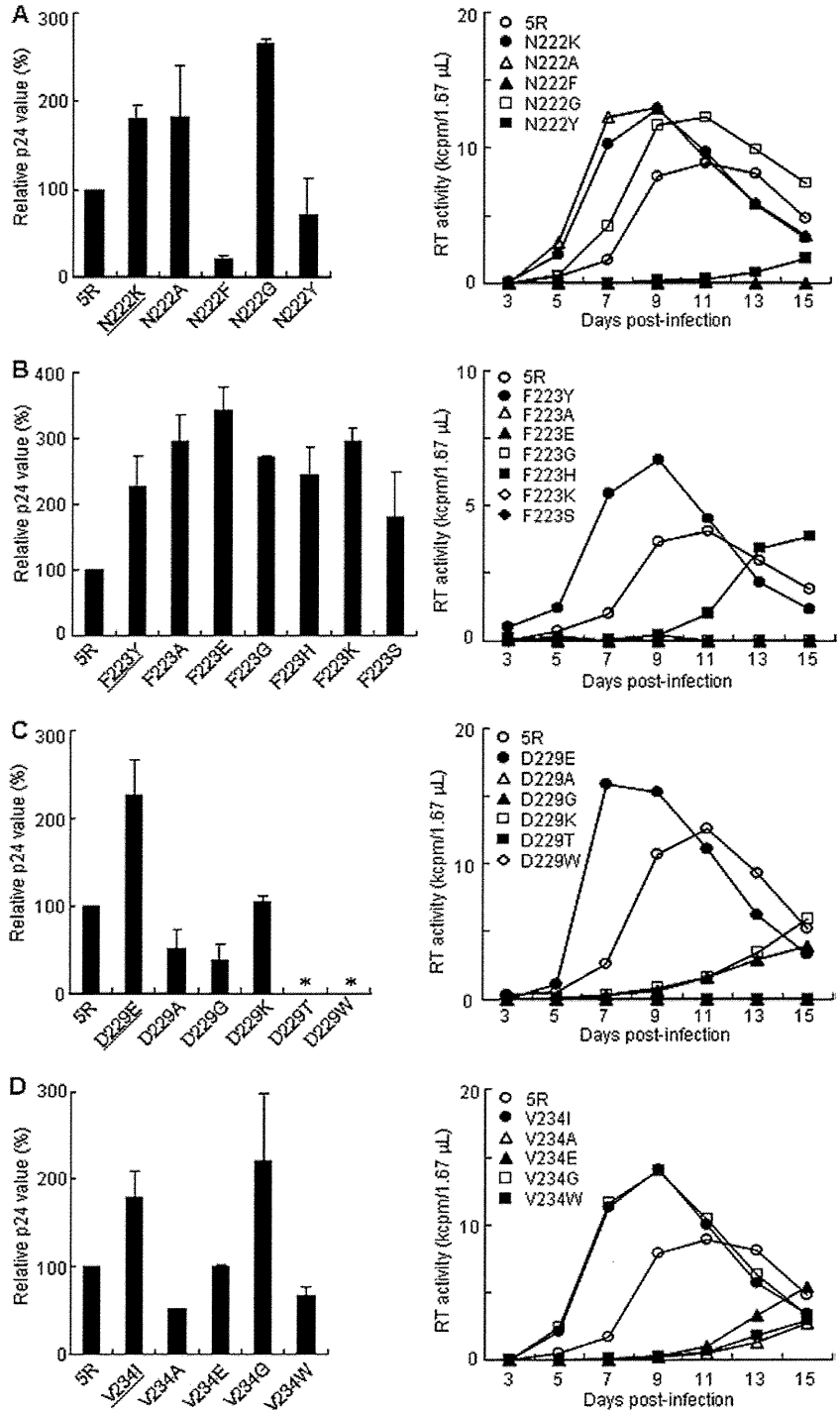

FIG 3 Effect of various amino acid substitutions at the N222 (A), F223 (B), D229 (C), and V234 (D) sites in the *Pol*4889-4923 region on virion production and replication kinetics. Details of the substitution for each mutant are shown in Table 1. Left panels, virion production. M8166 cells were cotransfected with the indicated *env*-deficient proviral clones and a luciferase reporter vector (pGL3) by using a Nucleofector. Virion amounts in the culture supernatants on day 2 posttransfection were measured. The amount of p24 was normalized by luciferase activity in cell lysates. The amount of p24 relative to that produced by 5R is presented. Mean values ± SD from at least two independent experiments are shown. Results for N222K, F223Y, D229E, and V234I shown in Fig. 2D (underlined) are incorporated into each panel for an easy comparison. *, under the detection limit. Right panels, viral replication kinetics. Viruses were prepared from transfected 293T cells, and equal amounts were inoculated into M8166 cells. Virus replication was monitored by RT activity released into the culture supernatants. Data in panels A and D were obtained from the same experiment, and the same result for 5R is shown separately in panels A and D as a control. Representative data from three independent experiments are shown.

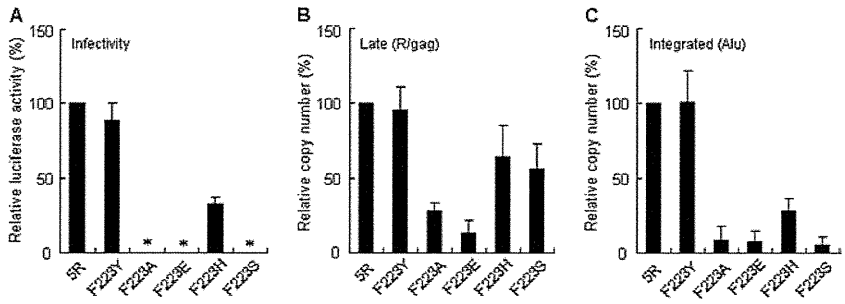

FIG 4 Effect of various amino acid substitutions at the F223 site on the early viral replication phases. (A) Single-cycle viral infectivity. VSV-G-pseudotyped viruses were prepared from transfected 293T cells, and equal amounts were inoculated into M8166 cells. Cells were collected and lysed on day 1 postinfection for luciferase assays. Infectivity is presented as luciferase activity relative to that exhibited by 5R. Mean values ± SD from at least four independent experiments are shown. *, mean values are <0.1%. (B and C) Monitoring viral cDNA synthesis. VSV-G-pseudotyped viruses from transfected 293T cells were treated with DNase I, and equal amounts were inoculated into M8166 cells. Total DNA was extracted from infected cells on day 1 postinfection and subjected to real-time quantitative PCR analyses with primer pairs specific for the late (B) and integrated (C) forms of viral cDNA. The DNA copy number relative to that of 5R is presented. Mean values ± SD from at least four independent experiments are shown.

naturally occurring synonymous polymorphism in some genes can influence the expression levels, structures, and functions of their encoded proteins (42–44). In addition, the IN CTD sequence is more heterogenous than those of the other IN domains (15, 17, 19). To clarify the significance of the nucleotide sequence in the *Pol*4889-4923 region for viral replication, we examined HIV-1 sequences within the region obtained from the HIV Sequence Compendium (Los Alamos National Laboratory, NM, USA). As shown in Table 2, while viruses carrying F223Y or D229E, which we identified as growth-enhancing mutations, were not found, those with N222K or V234I were present. We noted that codon variants with distinct growth abilities, V234I (ATT) and V234I-2 (ATC), coexisted in a viral population with different frequencies (Table 2). This suggested that there may be natural variants of HIV-1 with distinct replication potentials. Moreover, a sequence comparison in the *Pol*4889-4923 region revealed the presence of natural synonymous variations for parental clone 5R-encoded amino acid residues, even though the frequency was lower than that of 5R (Table 2). Thus, we examined whether viral replication can be affected by natural synonymous changes at the sites of adaptive mutations (N222, F223, D229, and V234) as well as other sites (V225, Y226, and P233) within the *Pol*4889-4923 region. The viral growth kinetics of 5R and its natural variants at adaptive mutation sites (N222aac, F223ttc, D229gat, and V234gtg) were determined in human MT4/CCR5 cells (Fig. 7A and Table 2). While N222aac and F223ttc exhibited growth kinetics similar or slightly better than those of 5R, the viral replication potentials of D229gat and V234gtg was markedly higher and lower, respectively, than that of 5R (Fig. 7A and Table 2). We next determined the viral growth kinetics of additional natural synonymous variants (V225gtc, Y226tac, and P233cct/ccc/ccg). Alterations in the viral replication potentials of these clones were evident: the viral replication kinetics of V225gtc were similar to those of 5R, whereas growth ability was higher for Y226tac and lower for P233cct/ccc/ccg than for 5R (Fig. 7B and Table 2). On the other hand, the genome structure of 5R is different from that of natural human-tropic HIV-1 due to the change of the cyclophilin A-binding loop-coding region in *gag* and of an entire *vif* to the corresponding regions of SIVmac239 (34). Thus, we determined whether these natural synonymous variations also affect the viral replication of human-tropic HIV-1 (NL4-3 clone). The viral growth potential of NL4-3 was altered similarly as that of 5R by natural synonymous changes: the replication abilities of D229gat and Y226tac were higher than that of NL4-3, and those of V234gtg and P233cct/ccc/ccg were lower than that of NL4-3 (Fig. 7C and D). We conclude from these results that natural variations (single-

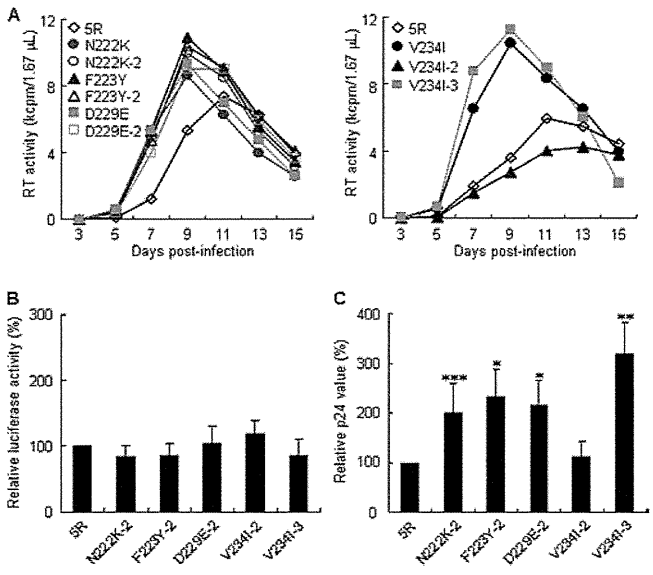

FIG 5 Effect of codon alterations at N222K, F223Y, D229E, and V234I sites on different stages of viral replication. N222K-2, F223Y-2, D229E-2, V234I-2, and V234I-3 indicate mutant clones containing an altered codon. The codon used for each mutant is shown in Table 1. (A) Viral replication kinetics. Input viruses were prepared from transfected 293T cells, and equal amounts were inoculated into M8166 cells. Virus replication was monitored by RT activity released into the culture supernatants. Representative data from at least two independent experiments are shown. (B) Single-cycle viral infectivity. VSV-G-pseudotyped viruses were prepared from transfected 293T cells, and equal amounts were inoculated into M8166 cells. Cell lysates were prepared on day 1 postinfection and subjected to luciferase assays. Infectivity is presented as luciferase activity relative to that exhibited by 5R. Mean values ± SD from at least three independent experiments are shown. (C) Virion production. M8166 cells were cotransfected with the indicated *env*-deficient proviral clones and a luciferase reporter vector (pGL3) by using a Nucleofector. Virion production on day 2 posttransfection was measured by the amount of p24 in the culture supernatants. The amount of p24 was normalized by luciferase activity in cell lysates. The amount of p24 relative to that produced by 5R is presented. Mean values ± SD from at least three independent experiments are shown. Significance relative to 5R as calculated by the Student *t* test is shown (*, $P < 0.01$; **, $P < 0.05$; ***, $P < 0.1$).

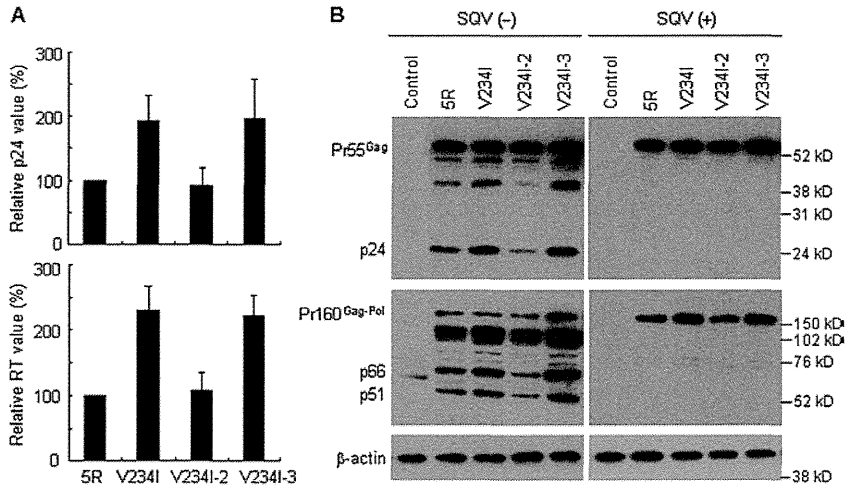

C

	SQV (-)			
	Actin	p24	p66	p51
Control	0.98 ± 0.10	NA	NA	NA
5R	1.00 ± 0.00	1.00 ± 0.00	1.00 ± 0.00	1.00 ± 0.00
V234I	1.18 ± 0.12	2.65 ± 0.42	1.58 ± 0.17	2.55 ± 0.24
V234I-2	1.25 ± 0.13	0.30 ± 0.20	0.32 ± 0.14	0.25 ± 0.15
V234I-3	1.10 ± 0.07	3.07 ± 0.26	3.08 ± 0.71	3.91 ± 0.37

	SQV (+)		
	Actin	$Pr55^{Gag}$	$Pr160^{Gag\text{-}Pol}$
Control	0.85 ± 0.11	NA	NA
5R	1.00 ± 0.00	1.00 ± 0.00	1.00 ± 0.00
V234I	0.94 ± 0.19	1.22 ± 0.13	1.73 ± 0.10
V234I-2	1.03 ± 0.28	0.73 ± 0.18	0.61 ± 0.11
V234I-3	0.90 ± 0.16	1.34 ± 0.19	1.84 ± 0.17

FIG 6 Effect of codon alterations at the V234I site on intracellular viral protein expression. (A) Expression levels of Gag-p24 and Pol-RT as determined by ELISA. 293T cells were transfected with the indicated proviral clones, and on day 2 posttransfection, lysates were prepared from transfected cells for the analysis of Gag-p24 and Pol-RT. The amounts of Gag-p24 and Pol-RT relative to those expressed by 5R are presented. Mean values ± SD from three independent experiments are shown. (B) Expression pattern of viral proteins as analyzed by Western blotting. 293T cells were transfected with the indicated proviral clones in the absence (−) or presence (+) of 2 μM SQV. Cell lysates were prepared from transfected cells on day 1 posttransfection, and analyzed by Western blotting using anti-p24 (upper panels), anti-RT (middle panels), and anti-β-actin (lower panels) antibodies. The migration positions of mass standards are indicated on the right. Representative data from two independent transfection experiments are shown. Control, pUC19. (C) Quantitative analysis of the Western blot. Signal intensities of viral proteins were quantitated, and the intensities relative to those with 5R proteins are shown. Mean values ± SD obtained from the two independent transfection experiments in panel B are indicated. NA, not applicable.

nucleotide synonymous mutations) in the 3′ region of the HIV-1 *pol* gene (nt 4889 to 4923 for 5R and nt 4895 to 4929 for NL4-3) can alter viral replication potential.

Natural synonymous changes influence the expression levels of intracellular viral proteins (Gag, Gag-Pol, Vpu, and Env) but not those of Nef and Rev. Gag/Gag-Pol expression levels in V234I codon variants varied correlatively with their virion production/replication abilities (Fig. 5 and 6). Env, in addition to Gag/Gag-Pol, is of course required for infectious virion formation. HIV-1-encoded proteins are translated from distinct viral mRNA species, and the regulation of gene expression is different for early transcripts (completely spliced form) and late transcripts (singly spliced and unspliced forms). To investigate further the virological effect of single-nucleotide natural variations, we determined the expression levels of products from various mRNA species: Gag and Gag-Pol from the unspliced form, Vpu and Env from the singly spliced form, and Nef and Rev from the completely spliced form. Proviral clones (5R, Y226tac, D229gat, P233ccc, V234I, and V234gtg) were transfected into 293T cells, and cell lysates prepared on day 1 posttransfection were analyzed by Western blotting. Although V234I was not a synonymous change in the *Pol*4889-4923 region, this clone was included in this analysis because V234I is a single-nucleotide natural variant of V234 in 5R, and its virion production/replication ability was increased or decreased by single-nucleotide substitutions at this position (Table 2). As shown in Fig. 8A, we confirmed that virion production levels in transfected 293T cells correlated with viral replication potential (Fig. 2, 7, and 8A) (upregulated, Y226tac, D229gat, and V234I; downregulated, P233ccc and V234gtg). We then examined the intracellular expression level of each viral protein (Fig. 8B).

TABLE 2 Amino acid/codon frequency in the 3′ region of the *pol* gene (nt 4889 to 4923 for 5R and nt 4895 to 4929 for NL4-3) of HIV-1/SIVcpz[a]

Amino acid position in IN	Amino acid frequency[b]			Codon frequency[b]			
	Amino acid	No.	%	Codon	No.	%	Growth[c]
222	N[d]	179	91.3	AAT[d]	175	89.3	++
				AAC	4	2.0	++/+++
	K[e]	14	7.1	AAA[e]	14	7.1	+++
	Q	2	1.0	CAA	2	1.0	ND[f]
	D	1	0.5	GAT	1	0.5	ND
223	F[d]	196	100.0	TTT[d]	183	93.4	++
				TTC	13	6.6	++/+++
	Y[e]	0	0.0	TAT[e]	0	0.0	+++
225	V[d]	195	99.5	GTT[d]	175	89.3	++
				GTC	20	10.2	++
	L	1	0.5	CTT	1	0.5	ND
226	Y[d]	194	99.0	TAT[d]	193	98.5	++
				TAC	1	0.5	+++
	F	1	0.5	TTT	1	0.5	ND
	H	1	0.5	CAT	1	0.5	ND
229	D[d]	196	100.0	GAC[d]	194	99.0	++
				GAT	2	1.0	+++
	E[e]	0	0.0	GAA[e]	0	0.0	+++
233	P[d]	194	99.0	CCA[d]	135	68.9	++
				CCT	35	17.9	+
				CCC	23	11.7	+
				CCG	1	0.5	+
	S	1	0.5	TCA	1	0.5	ND
	T	1	0.5	ACC	1	0.5	ND
234	V[d]	26	13.3	GTT[d]	25	12.8	++
				GTG	1	0.5	+
	I[e]	128	65.3	ATT[e]	127	64.8	+++
				ATC	1	0.5	+
	L	40	20.4	CTT	39	19.9	ND
				CTG	1	0.5	ND
	S	1	0.5	AGC	1	0.5	ND
	T	1	0.5	ACT	1	0.5	ND

[a] For 196 sequences of HIV-1/SIVcpz complete genomes from the HIV Sequence Compendium, 2011 (Los Alamos National Laboratory; http://www.hiv.lanl.gov).
[b] Relative to 196 sequences of HIV-1/SIVcpz strains.
[c] +++, replication peaked earlier or virus production levels on the peak day were higher than those of the parental clones; ++, replication kinetics were similar to those of the parental clones; +, replication peaked later or virus production levels on the peak day were lower than those of the parental clones. Data were obtained in M8166 or MT4/CCR5 cells.
[d] Amino acid encoded or codon usage in parental clones.
[e] Amino acid encoded or codon usage in adapted (growth-enhanced) viruses.
[f] ND, not done.

The intracellular expression levels of Gag, Gag-Pol, Vpu, and Env varied among the clones tested and correlated with viral replication potential: clones with enhanced growth efficiencies expressed higher levels of these proteins, and vice versa (Fig. 2, 7, and 8B and C). In contrast, the expression levels of Nef and Rev by all proviral clones tested were similar to that of 5R, and they were constant for all variants with different virion production/replication potentials (Fig. 2, 7, and 8). Furthermore, Tat activity was determined by cotransfection assays with 5R, its single-nucleotide variants, and the 5RLTR-Luc reporter construct. No significant difference in the abilities of these proviral clones to *trans*-activate luciferase gene expression was observed, which indicated that 5R and its variants had similar Tat activity (Fig. 8D). These results suggest that single-nucleotide changes in the *Pol*4889-4923 region can alter virion production/replication potential by modulating the expression levels of late (but not early) viral proteins.

Naturally occurring single-nucleotide variations change the expression patterns of HIV-1 mRNA species. Naturally occurring single-nucleotide mutations that alter the expression levels of viral late proteins were Y226tac, D229gat, V234I, P233ccc, and V234gtg (Fig. 8). We noted that these mutations clustered in the region proximal to the splice acceptor A1 (SA1) site (designated SA1prox in Fig. 9A). To determine the mechanistic basis for the altered phenotype, we analyzed the effect of single-nucleotide changes on the profiles of viral mRNA expression. 293T cells were transfected with parental clones (5R and NL4-3) or their mutants,

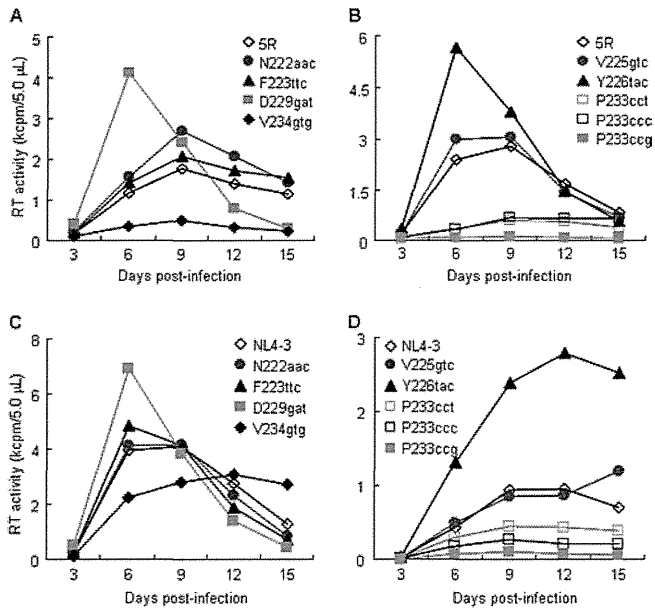

FIG 7 Effect of single-nucleotide synonymous changes in the *Pol*4889-4923 region on viral replication potential. Viruses were prepared from transfected 293T cells, and equal amounts were inoculated into MT4/CCR5 cells. Virus replication was monitored by RT activity released into the culture supernatants. Representative data from two independent experiments are shown.

and DNase I-treated poly(A)$^+$ RNAs were prepared from total cell RNAs at 10 to 20 h posttransfection. Northern blot analysis of these samples using a probe (U probe) to detect all HIV-1 mRNA species (Fig. 9B) was then performed (Fig. 9C). Because no significant difference in the RNA expression patterns for the samples of each clone prepared at 10 and 20 h posttransfection was noted (data not shown), we comparatively analyzed viral mRNAs in cells at the latter time point. As shown in Fig. 9C, the expression levels of viral late proteins did not directly correlate with the steady-state levels of their respective transcripts (9 kb and 4 kb) (Fig. 8B and 9C, left panel). The total amounts of viral mRNAs, especially the 1.8-kb mRNA species, were lower for the clones with increased viral late protein expression (Y226tac, D229gat, and V234I) than for 5R and the other mutants (P233ccc and V234gtg). However, single-nucleotide mutations always gave unique viral mRNA expression profiles. Several bands (*1 to *4 in Fig. 9C, left panel) other than the three major viral RNA species (1.8 kb, 4 kb, and 9 kb) were more or equally intense for P233ccc and V234gtg, with the poor expression of late proteins, and less intense for Y226tac, D229gat, and V234I, with the high expression of late proteins, than for 5R. Similar results, albeit to a lesser extent, were obtained for NL4-3 and its mutants with higher or lower abilities to replicate in cells (Fig. 9C, right panel). As such, viruses with a relatively high replication ability in each group (5R and NL4-3) appeared to be tuned up to have three major mRNA species. Northern blot analysis using HeLa cells was performed to exclude the possibility that the viral mRNA expression pattern described above was 293T cell specific. Results similar to those in 293T cells were obtained for 5R, NL4-3, and their mutants (D229gat and V234gtg) (data not shown). Taken together, our results here show that single-nucleotide changes in the SA1prox affect the expression patterns of viral mRNA species and suggest that this transition may lead to the enhancement or reduction in viral late protein expression/replication efficiency.

To identify the nature of transcripts detected as extra bands (*1 to *4) (Fig. 9C), we performed Northern blot analysis using RRE, vif, and vpr probes (Fig. 9B). As expected, 9-kb transcripts but not 1.8-kb transcripts were detected by the RRE, vif, and vpr probes (Fig. 9D). While all transcripts longer than 4 kb were detected by the RRE probe, the vif and vpr probes recognized the species *1 to *3 and *1 to *4, respectively. The *2 band was more intense with the vpr probe than with the vif probe. Thus, the *1 species contained the *vif* transcript (Fig. 9B), and the *2 band consisted mainly of the *vpr* transcript (Fig. 9B). Transcripts *3 and *4 contained the Vif/Vpr-coding region and Vpr-coding region, respectively, without the RRE region.

Northern blot analysis revealed that the lower expression of late proteins by 5R, P233ccc, and V234gtg was linked to the abundance of transcripts, especially the *1 and *3 species. We hypothesized that these abundant transcripts may disturb the expression of late proteins. To test this possibility, we performed interference assays by the cotransfection of D229gat and 5R/V234gtg (Fig. 10). If the extra transcripts *1 and *3 interfere with translation from transcripts corresponding to late proteins, the Gag-p24 expression levels of D229gat would be proportionally decreased upon cotransfection with increasing amounts of 5R or V234gtg. As shown in Fig. 10 (top and middle panels), p24 expression levels were increased in cells upon single transfection of D229gat, 5R, or V234gtg with an increasing DNA amount, and marked differences were observed between each clone (D229gat > 5R > V234gtg). When a constant amount of D229gat and an increasing amount of 5R or V234gtg were cotransfected, p24 expression levels reflected just the addition of the amount produced by each clone. Virion production from cells correlated well with the intracellular p24 expression levels (data not shown). Cotransfection assays using D229gat and the *gag/gag-pol* frameshift mutant of V234gtg (gtg-Spe), which is incapable of producing p24, were performed to confirm this result. As is clearly observed in Fig. 10 (bottom panel), the increase in the amount of the gtg-Spe clone did not affect p24 expression levels produced from D229gat. Taken together, these results suggest that a large amount of transcripts (especially the *1 and *3 species) in 5R and V234gtg clones does not interfere with Gag-p24 expression and also that the single-nucleotide changes in the SA1prox act on the expression of late proteins in *cis*.

DISCUSSION

In this study, we demonstrated that four adaptive mutations in the 3′ region of the *pol* gene encoding IN upregulated the viral replication potential by increasing virion production levels without any effects on the early replication phase (Fig. 2). Moreover, the identification of V234I codon variants that have different abilities to produce virions and replicate in cells suggested regulation by single-nucleotide changes (Fig. 5). A comparative investigation of nucleotide sequences in the 3′ region of the *pol* gene (nt 4889 to 4923 for 5R and nt 4895 to 4929 for NL4-3) has revealed that these variants naturally coexist in a viral population (Table 2). We show here that naturally occurring synonymous changes (Y226tac, D229gat, P233cct/ccc/ccg, and V234gtg) can alter the viral replication potentials of HIV-1 5R and NL4-3 (Fig. 7 and Table 2).

The naturally occurring single-nucleotide variations that alter viral replication potential clustered in the SA1prox (Fig. 9A).